Journal of Traffic and Transportation Engineering 5 (2017) 171-202
doi: 10.17265/2328-2142/2017.04.001

Procedure for a Temperature-Traffic Model on Rubberized Asphalt Layers for Roads and Railways

Fernando Martínez Soto and Gaetano Di Mino

Department of Civil and Environmental Engineering, Aerospace & Materials (UNIPA), Scuola Politecnica—Università degli Studi di Palermo (UNIPA), Viale delle Scienze, Ed. 8, 90128 Palermo, Italy

Abstract: The impact of temperature on the mechanical properties and thermal susceptibility of the railway bituminous sub-ballast layer, has served as motivation to develop the advanced measurement of thermal cycles in this layer and, an evaluation of the average seasonal temperatures interpolated by sinusoidal functions, of which characteristic parameters are determined. According to weather situation, Barber's temperature model was used to prove the effectiveness for the railway superstructure. It is included the assessment of improved modified asphalt mixes performed with coarse rubber from scrap tires, having 1.5 to 3 percent of crumb rubber (particle size 0.2-4 mm) by weight of the total mix, as sub-ballast layer in railway and base layers on roads, recurring to the Superpave mix design compaction enhanced after computer simulations to evaluate real stresses derived from the rail traffic and climatic conditions. This article following the assessment of the average seasonal temperatures, involves the characterization of rubberized materials with attention to crumb rubber properties, designed with dry technology, to enhance the bitumen-rubber and binder-voids ratios. Indirect tensile strength and water sensitivity tests were applied for the evaluation of its mechanical properties including dynamic complex modulus at elevated temperature to measure the amount of bitumen absorbed by the rubber. The rubberized mix-results obtained and the comparison with a conventional HMA (hot mix asphalt) show that these dry rubber bituminous mixtures are particularly effective in damping vibrations. The purpose of using rubber modifiers in hot mix asphalt to obtain a stiffer-elastic sustainable material has been achieved for the assessment of its behavior in sub-ballast/base layers.

Key words: Superpave, rubber-modified asphalt, bituminous mixtures, temperature, compaction, sub-ballast, railway, indirect tensile strength, trackbed design.

Highlights

- An innovative approach for the volumetric design of bituminous mixture with rubber (dry process);
- Optimal parameters of temperature and traffic to characterize the mixture for a sub-ballast layer;
- Applicability of Barber forecasting model used in the field road, to the railway superstructure;
- Performance of the design process for the volumetric analysis of rubberized asphalt;
- 160 kN and 80 kN, respectively, rail equivalent axle load (R_{ESAL}) were selected comparing sub-ballast vs. road base course solicitations induced for each layer;
- Increase of workability and compaction properties decreasing air voids content to 3%-4% of the total mix weight;
- Crumb rubber percentage between 1.5% to 2% and a digestion time of 120 min produced the optimal results.

1. Introduction

Sub-ballast layer is a key element of the track and its performance dramatically affects the reliability and durability of the whole infrastructure, which plays a vital role as a foundation for the superstructure (i.e., rails, sleepers, and ballast) and carries the vehicle loads to the ground [1].

The blanket is a layer, or several layers, of granular material laid over the subgrade which conforms and creates its desired properties. Frequently, unbound granular materials are replaced by bituminous sub-ballast, being almost completely water-resistant,

Corresponding author: Fernando Martínez Soto, Ph.D.; research fields: asphalt materials, transports, construction, civil engineering, architecture, and environmental sustainability. E-mail: arquinandoms@gmail.com.

that may provide additional benefits to the subgrade protection and track performance (Fig. 1).

This has an important effect on slowing down the deterioration process over the track's service life [2]. The bituminous sub-ballast is composed of a dense-graded bituminous mixture similar to the base course for road pavements [3]. The bitumen in the sub-ballast is normally increased to 0.5% compared to the base layer and the air voids decreased to 1%-3% to enhance the impermeability of the layer [4]. This results in a mixture characterized by a medium permanent deformation resistance. However, rutting does not represent a main concern in the track-bed because the presence of the ballast distributes pressures of axle loads over a wider area.

Other studies have observed that the use of HMA as a sub-ballast allows for a reduction in vibration levels throughout the track, therefore reducing noise [5].

Considering these aspects, the use of bituminous sub-ballasts improves the track quality and durability (higher protection of the subgrade in terms of load dissipation). This leads to reduced maintenance interventions, improving adherence to track geometric parameters [2].

1.1 Advantages of Bituminous Sub-ballast

Traditional railway track generally consists of rails, sleepers, fastenings, ballast and a formation layer over the ground. The characteristics of materials and the thickness of the layers composing the railway track structures are very often assigned by practice [6]. The constant demand in high speed and loading capacity increasing, involve the incorporation of the required sub-ballast layer. The thickness of granular layers between sub-ballast and ground has been increased in modern tracks with the aims of obtaining higher bearing capacity, quality and durability of the system [7]. With this same objective, other configurations such as track with bituminous sub-ballast are becoming widely used in the construction of new railway lines all around the world [3, 8]. About this trend, it should be also considered that all these changes in the railway section lead, in addition to the increase in bearing capacity, to the modification of other important track parameters such as the vertical stiffness [9], defined as the ratio between a vertical track load and the track deflection caused by the load.

In the case of ballasted tracks, sub-ballast layers are determining elements in the mechanical performance of the track and for the protection of the ballast. Using bituminous mixtures for sub-ballast layers has been identified as a possible solution for the necessary enhancement of the track structure.

A substantial amount of this development research has been conducted during the past 25 years [10].

Asphalt underlayment has shown to be applicable to track features with weak subgrades, soft soils and poor drainage. From a theoretical and mechanical consideration, the effects of sub-ballast layer can be related easily to the main track design parameters [11]:

- Vertical stresses on the ballast (permanent deformation and possible track settlement as indicators of posterior maintenance needs);
- Horizontal tensile strains on the sub-ballast (as an indicator of fatigue effects and reduction of service life);

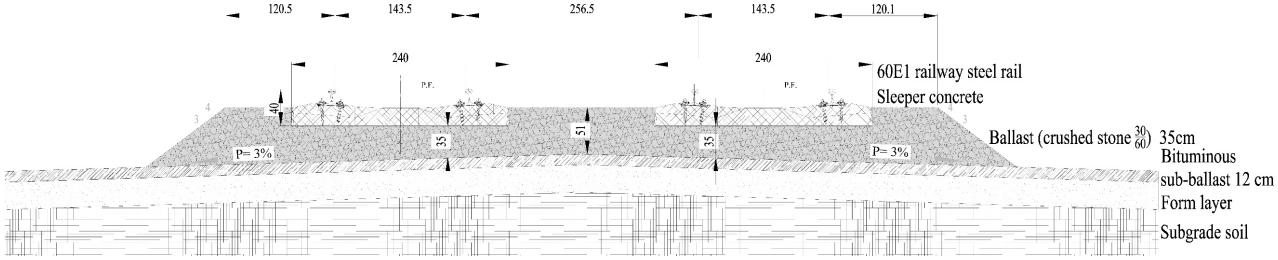

Fig. 1 Section through railway track showing the sub-ballast and formation layers.

• Vertical stresses on the sub-grade (as an indicator of subgrade long-term performance and track maintenance costs).

1.2 Analyzing the Conditioning Factors

The performance of asphalt pavements is greatly influenced by temperature distribution and environmental conditions to which it is exposed.

Barber [12] observed that pavement temperature fluctuations roughly followed a sine curve with a period of one day. A good estimation of asphalt surface temperature was observed by including both the solar radiation and the air temperature in the model.

Pavement temperatures are of interest linking with the stabilization, curing and moisture movements of bituminous sub-ballast layers [12].

Straub et al. [13] developed a computer model to predict pavement temperatures based on air temperature and solar radiation. It was found that the surface temperature measurements need to be made at the surface to achieve a good correlation with solar radiation. Also, the pavement temperatures at various depths of an asphalt pavement were found to be independent of the thickness of the asphalt pavement. Furthermore, the results indicated that solar radiation had a greater effect on pavement surface temperatures than air temperatures.

Williamson [14] developed a model to predict pavement temperature at various depths using finite difference techniques. Inputs for the model included climatic parameters as well as the thermal properties of the pavement. One of the most important environmental factors that significantly affect the mechanical properties of asphalt mixtures is temperature [15]. Thus, accurate prediction of the temperature distribution within the pavement structure is important.

The properties of asphalt mixtures change significantly with temperature variation. Bituminous mixtures suitable for railway sub-ballast are often brittle and susceptible to cracking at low temperatures, in addition to being prone to permanent deformation at high temperatures.

Precise prediction of asphalt pavement temperature at different depths based on air temperature measurements can help engineers to perform retroactive calculations of the bituminous mixtures module and to estimate pavement deflections [16].

Temperature is very important to the selection of the long-term grade performance values of the pavement. As HMA is a viscoelastic material, the structural or load-carrying capacity of the pavement varies with temperature [17]. The bearing capacity of each layer is influenced by climatic conditions regarding two different aspects [18]:

• Thermal regime, in relation to the thermal susceptibility and the thermal behavior to the generated deformations in the cement bound materials;

• Moisture regime, in relation to the influence of water content on the physical and mechanical properties of the granular materials.

So, climatic factors that may influence the pavement thermal regime of the railroad are air temperature, solar radiation, and wind speed.

1.3 Optimizing of Rail Track Design

The railway structure seeks to optimize a reliable performance, the thickness of each layer to withstand allowable stresses throughout the railroad track and contain the deformation due to traffic loads and temperature oscillations. In this way, the properties of the material must be defined by layers, optimizing according to their mechanical behaviour, which compose the structure of the track, both to verify the resistance to fatigue common in the railroads and to calculate the permissible deformations in high structures speed.

In fact, by changing the characteristics of the materials constituting the railway sub-structure, the size of the structure and maintenance costs are increased due to induced stresses from railway traffic and consequent deformations [19].

The use of different types of sub-ballast (granular or bituminous) caused low variations in bearing capacity, while the incorporation of an elastic layer as rubberized asphalt under the sub-ballast causes an important reduction in the bearing capacity of the system, being more remarkable when softer elements are used.

2. Problem Statement 01

2.1 Background of Temperature Profile Models

Some of the temperature models are based on mechanistic methods, energy balance and finite difference equations, whereas others are purely empirical regressions [20]. A mechanistic method is structured in the identification and collection of input data, the calculation of the stresses and strains in all layers and, finally, on determining the design life considering the most critical conditions.

The widespread use of computer programs with widely validated theoretical models has now led to misgivings about experimental methods. The modifications include the incorporation of current best practices and presenting the engineer with guidelines on how to determine input parameters, which are normally difficult to obtain [21].

The inputs required for the model included the shortwave and long-wave back radiation, convection, air temperature, material unit weight, moisture content, material classification, thermal conductivity, and heat capacity of the pavement material.

A simulation model that predicts pavement temperatures during summer condition based on the finite difference approximation of the heat transfer equation was presented by Hermansson [22]. Input data to the model are hourly values for solar radiation, air temperature and wind velocity. A good agreement between the measured and calculated temperatures was observed. The solar radiation and the depth within the pavement were also incorporated.

Ferreira et al. [23] analysed through an FEM (finite-element model), the long-term deformational behaviour of the subgrade, to assess the effect of different solutions in the performance of railway track-bed layers resulting from environmental effects (atmospheric actions and phreatic level variations) when modelling superficial drainage systems that enable the runoff of excess rainwater.

The advent of the Superpave (Strategic Highway Research Program) steered research in a slightly different direction. The performance-type specifications developed for asphalt cements required that a certain grade of asphalt binder perform over a given range of temperatures. For pavement engineers, knowing the upper and lower temperatures that a pavement would be exposed to became important.

2.2 Considerations for Railways

The primary modes of heat transfer are incident solar radiation, thermal and longwave radiation between the railway surface and the environment, convection due to heat-transfer between the pavement surface and the air fluid that is in contact with the surface, and conduction inside the pavement.

After these considerations, an assessment of the thermal model developed to predict max/min temperatures on the railway trackbed is necessary.

Among the most common measures, we considered temperature, relative humidity, atmospheric pressure, wind speed, wind direction, precipitation, and hours of sunlight [24]. The selected typical 12 months were chosen from statistics determined by using five elements: global horizontal radiation, direct normal radiation, dry bulb temperature, dew point temperature, and wind speed. These elements are considered the most important for simulation of solar energy conversion systems and building systems.

Crispino [25] measured the thermal fluctuations of sub-ballast layer, to evaluate the average seasonal temperature. It is of interest to investigate, compare, and assess the performance of his proposed model based directly on a realistic correlation between climatic conditions at a given location and sub-ballast performance (the analysis included the solar radiation

and air temperature providing reasonable estimates of surface temperatures).

2.3 Objectives

A complex study has been developed that covers two different but parallel aspects for the characterization of bituminous mixtures in the railway sub-ballast.

The present study, therefore, is divided in a first part, that studies the aspects of traffic and temperature by means of modelling with the aim of representing the real conditions in that layer of the rail profile and, a second part, that represents the mix-design (volumetric criteria and post-compaction) of the mixtures in the laboratory using the Superpave compaction technique, developed in this work exclusively for the railway sector, since until now it is applicable only on roads.

In this research, one of the crucial issues is to evaluate the distresses inside the railway section, especially the sub-ballast layer, regarding the prediction of temperature profile (from weather report and of design traffic-loads and number of repetitions) during the life-time. Numerous numerical models have been developed since the 1970s to address the mechanistic analysis of the railway track.

The analytical model to forecast temperatures proposed by Barber [12], which al-ready validated pavement structure, is used in this research to calculate rail stresses on railway track for the past three decades.

In this overall framework, attention must be paid to the bituminous materials. They are characterized by thermal susceptibility; thus, it is necessary to know the temperature within the layer and the relationship with the mechanical characteristics. In this paper, Barber's theory [12] was used to determine the temperature in the road base course, and the modifications purposed by M. Crispino were applied in the sub-ballast layer [26]. By means of a comparative analysis by simulating the thermal sub-ballast and road-base layer behaviour respectively, of known thermal properties, was possible to predict the maximum and minimum pavement temperatures, which obtained results are illustrated after different computer simulations, including the average seasonal temperature evaluation. It is shown to be well interpolated by sinusoidal functions, from which, the characteristic parameters are determined.

In the last chapter, is illustrated by an example that corresponds to three different traffic lines in the Sicilian traffic network (Palermo-Messina, Catania-Messina and, Siracusa-Catania main rail lines), and according to the Italian standard code for bituminous mixes in sub-ballast layer.

This research, after evaluating the optimal parameters of temperature and traffic that should characterize the optimum mixture for a sub-ballasted layer, in parallel, provides an advance in the development of a new methodology for the bituminous sub-ballast to adapt the Superpave mix-design approach (exclusively for roads) also to the railway system. The application of these procedure is needed for the Superpave mix-design of the underlayment in optimal conditions of manufacture.

For this purpose, a study was conducted with a hot mix asphalt conventional (unmodified mixture) and three different rubber modified asphalt concrete mixtures, performed with coarse rubber from scrap tires, containing 1.5 to 3 percent of crumb rubber (particle sizes between 0.2-4 mm) by weight of the total mix, as sub-ballast layer in railway and base layers on roads of similar characteristics, but which varied in type of coarse aggregates and amount of rubber used.

3. Methodology for a Temperature-Traffic Modellization

3.1 Track-Bed Model

The linear viscoelastic behavior of a bituminous mixture is a first step to the understanding of the elastic-plastic mechanical performance of high-speed line tracks with bituminous layers. Although its response is better described by viscoplastic constitutive laws accounting for temperature effects, for this

analysis is assumed a linear elastic model [27].

The dimensioning of the rail sub-ballast requires the determination of temperature in accordance with the prediction model reviewed. Due to the extensive tension analysis for the road model, as well as temperature studies for the tread layer, we have chosen to validate the railway model by adopting a multi-layer system that allows comparing the base layer and the sub-ballasted layer to stress-strain level.

The track system model is divided from top to bottom in rails, springs (tie plates/pads), ties, and layered support system components. Rail, pads and sleepers are modelled as prismatic elements with an isotropic linear elastic constitutive model by finite elements for trackbed design.

The railway and road structures are modelled as a multi-layer system from which the properties of each layer can be defined. The two sections (types and thicknesses of layers) and the solicitations points are shown in Fig. 2.

Fatigue cracking and rutting at low-high temperatures, respectively, are two of the most common causes of asphalt failure in flexible pavements [28]. Cracking of hot mix asphalt is not desirable because it causes the infiltration of water and the subsequent weakening of the subgrade.

It is therefore necessary to study the rail traffic (to determine the railway equivalent single axle load, R_{ESAL}), from a particular analysis of the geographical area where the infrastructure to be analyzed is located, and then depending on the climatic situation parameters, the stress-strain behaviour at the bottom of the base course and sub-ballast by performing several simulations is studied.

The minimum thickness of a hot mix asphalt sub-ballast layer will depend on the subgrade support. A poor subgrade requires a thicker sub-ballast, which can cause stress concentration and may not increase the fatigue life, so that it can be properly compacted.

3.1.1 Stress-Strain Behavior of Railroad Layers

Railway track structure can be calculated by elastic multi-layer theory, defining each layer by its thickness, elastic modulus and Poisson's ratio [29]. The pressure transmitted from trains by rail, sleepers and ballast can be considered uniformly distributed over a circular area (same vertical and shear stresses, same vertical and radial displacements).

Stresses and strains can be calculated in railroad materials for each layer of the track formation by means of structural analysis [30] and the finite element method, thus, tensions and deformations were calculated in every point of the trackbed [31] as shown in Fig. 3.

These values will then use for calculating the allowable number of load repetitions for fatigue verification in every point of the track-bed [32] of the railway track structure.

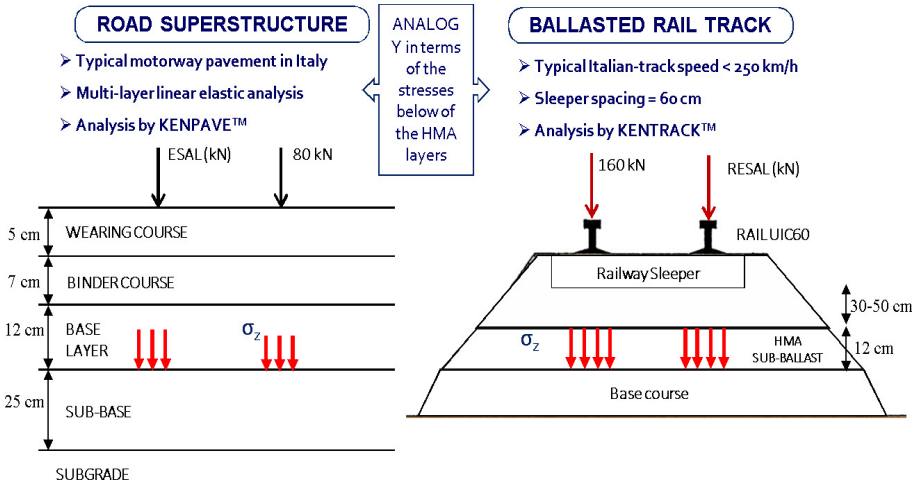

Fig. 2 Road and railway sections considered.

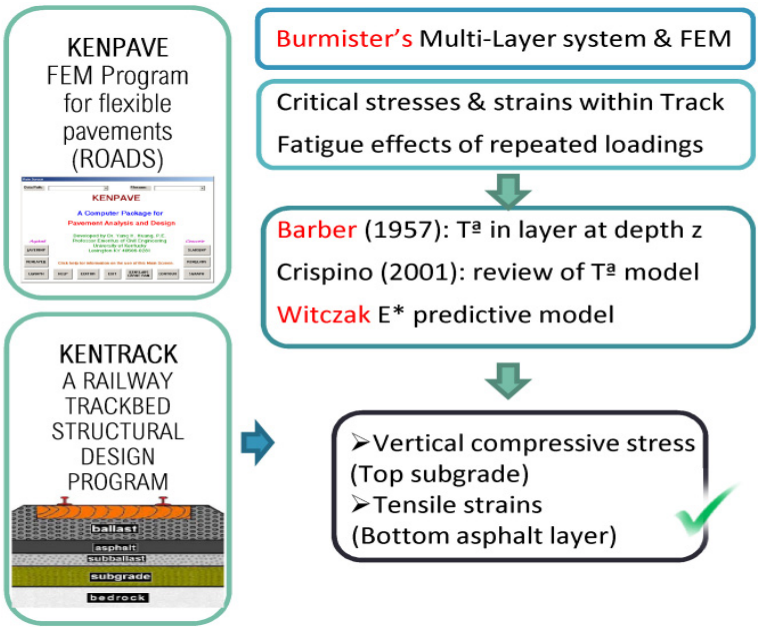

Fig. 3 Flow chart procedure for simulations.

KENPAVE® is a software that determines stress-strain-deformations in flexible-rigid pavements [33]. KENTRACK® is for the analysis and design of railway track-beds [4, 34-36], that provides a rational method for designing a railway track for different loadings and layer materials. It is a layer elastic finite element based computer program that can be utilized for a performance structural design and analysis of railroad trackbeds.

Kentrack, as a computer program for hot-mix asphalt in conventional ballast railways, determines the tensile strains at the bottom of the asphalt layer, a reliable indicative of potential fatigue cracking at low temperatures [10, 20, 34, 35, 37-39].

In order to find the standard axle load for railways that produces the same solicitations in road pavements, several simulations were run using both computer programs, considering a number of axle-passages between 80 kN (roads) until 200 kN (railways).

One hundred cycles were imposed to avoid the cumulative damage effect. The software simulations were carried out considering the air temperature equal to 0 °C (low temperatures representative) and 35 °C (high temperatures representative).

The horizontal tensile strains and the deflections produced in the road and railway structures were compared. The tensile strain at low temperature defines the railway equivalent single axle load (R_{ESAL}) because it is the critical factor governing cracking and fatigue.

The vertical displacement at high temperature is the factor that characterizes the permanent deformation or rutting. The results are shown in Fig. 4 and Table 1.

As it is possible to see from Fig. 3, the road deformations find the homologue for railways with an axle between 14 to 18 t, the average weight is equal to 15.98 t, thus 16 t has been selected as the reference R_{ESAL} for standard axle-rail predominant in the case study of Sicily. By chance, in the following section we see that this standard axle also concurs with the train model characteristic of the Italian railway lines.

3.1.2 Traffic Spectrum

The traffic information to be used for the thickness design includes the magnitude of wheel loads and the number of repetitions per year. The trains considered for the case study were high-speed trains that are operating on Italian lines.

The load for the conventional Italian passenger train consists of two (160 kN) wheels in a group on each side, spaced at 60 cm on rail. The loading system of the FEM model implemented in KENTRACK 4.0 [34]

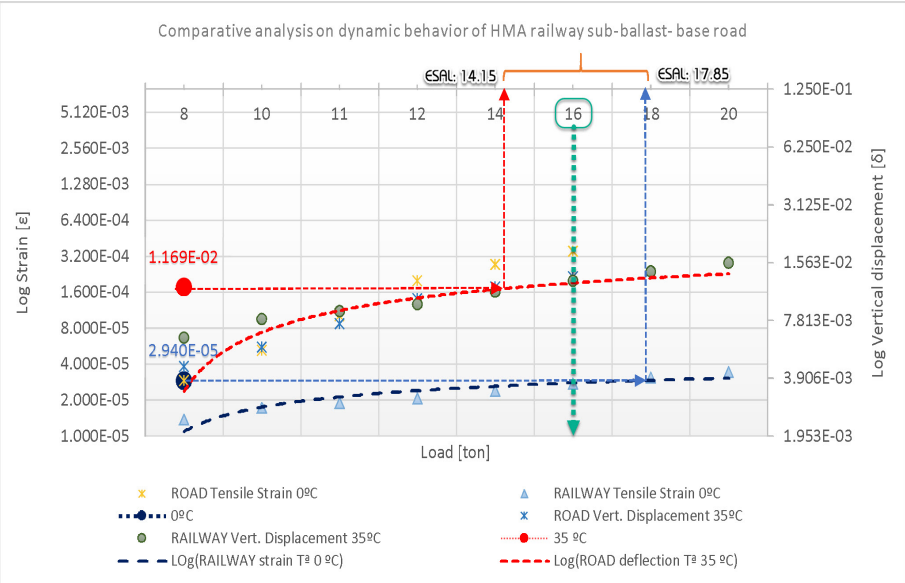

Fig. 4 Results obtained from the simulations carried out with KENPAVE and KENTRACK.

Table 1 Deformations results at 0 ºC and 35 ºC.

Pavement layer	Axle (t)	T^a (air temperature, ºC)	Tensile strain (εx)	Vertical displacement (δ)
Road (base layer)	8.2	0	2.940E-05	4.510E-03
Railway (sub-ballast)	8.0	0	1.380E-05	5.940E-03
	10		1.720E-05	7.400E-03
	11		1.900E-05	8.120E-03
	12		2.070E-05	8.840E-03
	14		2.410E-05	1.027E-02
	16		2.750E-05	1.169E-02
	18		3.110E-05	1.310E-02
	20		3.440E-05	1.450E-02
Road (base layer)	8.2	35	2.763E-05	1.169E-02
Railway (sub-ballast)	8.0	35	2.550E-05	6.390E-03
	10		3.190E-05	7.950E-03
	11		3.520E-05	8.720E-03
	12		3.840E-05	9.949E-03
	14		4.480E-05	1.103E-02
	16		5.130E-05	1.256E-02
	18		5.800E-05	1.409E-02
	20		6.440E-05	1.560E-02

was designed considering the long-distance intercity (Italian) train configuration, composed of 1 locomotive plus 4 bogies (16 axles) with a static load of 16 tons per axle and a distance between axles (wavelength of vibration) of 14.65 m. The running speed is between 200-250 km/h (56-70 m/s), diesel-electric, respectively, power, and 1.45 mm standard gauge. It is considered a frequency f, equal to the ratio between average train speed v, and wavelength λ, equivalent to 5 Hz (ratio between the maximum speed of a long-distance train 250 km/h or 69.45 m/s, and the wavelength characterized by the axle distance-tandem wheel, in this case, 14.65 m, where, $f = v/\lambda$ (see Fig. 5).

Because the critical strain and stress under the two wheels in one car are greater than those under four wheels in two adjoining cars, only two wheels are used

for the design purpose. For this purpose, it was necessary to define a complete set of information regarding all the components and the materials involved in the systems. In addition, selected parameters can be varied in magnitude and the relative influences evaluated.

Based on the standard input parameters, asphalt underlayment trackbeds can be analysed by varying parameters such as axle load, subgrade modulus, layer thickness, etc. The principal parameters (road-railway) used to create the reference sections are demonstrated in Tables 2 and 3.

3.1.3 Project Traffic of Rail Lines

The definition of project traffic must include a condition of effective loads and the number of movements of each train that will use the infrastructure during its useful life. Traffic forecasts should be referred to the various areas of the railway to differentiate the stress conditions to which each of them is subjected.

The amount of traffic is measured in terms of the number of repetitions of application of loads of different axles. So, the assessment of traffic implies knowledge of:

- the number of vehicles by year;
- the growth rate of the rail industry;
- the average number of axles/vehicle;
- the spectrum of axle loads;
- the transverse distribution of loads;
- the time horizon of the useful life;

Three different traffic lines in the Sicilian network were investigated and their traffic spectra were converted to RESALs (rail equivalent single axle loads). The frequency of the passage (f_k) of the k-axle load, defined as the ratio between the number of axle-steps and the total number of the axle-passages for 100 vehicles passing, is calculated using the following Eqs. (1)-(4):

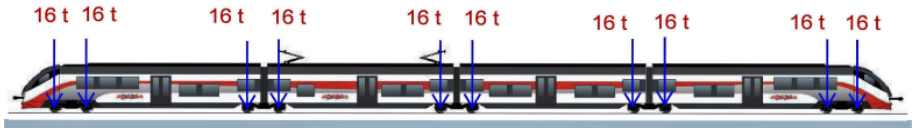

Fig. 5 Long distance intercity example train (250 km/h).

Table 2 Parameters selected for KENTRACK simulations.

Type of rail: 60E1 (UIC) 3141			Pandrol Fastclip system		
Young's modulus (MPa)	Limit of proportionality (MPa)	Limit of elasticity (MPa)	Static stiffness (MN/m)	Clamping force (kN)	Creep (kN)
192,000	500	600	> 150	> 16	> 9
Sleepers in PSC (Portland slag cement) wires					
Sleeper thickness (cm)	Sleeper width (cm)	Sleeper unit weight (g/cm)	Sleepers spacing (cm)	Length of sleeper (cm)	Rail distance (cm)
21	16.9	5.18	60	259	143.5
Type of axle considered for the simulations			Single		

Note: UIC = Union Internationale des Chemins de fer.

Table 3 Parameters selected for KENPAVE® simulations.

Road structure			
Material	Responses	No. of periods	No. of layers
Linear	Displacement	5	4
Load information			
Load	CR*	CP**	NR***
Single axle with single tire	12.62	800	1

*Contact radius of circular loaded areas (cm);

**Contact pressure on circular loaded areas (psi);

***No. of radial coordinates to be analysed under a single wheel (-).

$$T_D = 365 \quad T_{HV} \qquad r^{\,n} \qquad r \tag{1}$$

$$N_D = T_D \times (\sum_j^m f_j \times n_j) / \sum_j^m f_j) \times A \times Rt \tag{2}$$

$$A = \sum_k^m f_k \times (P_k / P_r)^g \tag{3}$$

$$f_k = \frac{\sum_i^j (f_j \times n_j)_i}{\sum_j^m \sum_i^j (f_j \times n_j)_i} x100 \tag{4}$$

where:

T_D = total number of load passages expected over the entire service life (-);

T_{HV} = average daily traffic in the year of the construction (-);

Rt = annual growth rate of traffic (-);

n = 30 years design life (year);

N_D = *RESAL*s at the end of the service life (-);

n_j = number of passages of the j-axle;

f_j = frequency of the j-axle;

P_k = k-axle load (kN);

P_r = axle load of the reference axle (kN);

A = coefficient of aggressiveness of railway traffic;

γ = coefficient for flexible bituminous railway and for flexible pavements (5-6, respectively); and

f_k = frequency of passage of the k-axle load (-).

An example, for a highway outside cities, the coefficient of aggressiveness, A, is around 1.57. For a main rail-line, the value obtained is around 0.30, considering the different γ coefficient, respectively, according to the 1993 AASHTO Guide for Flexible Pavement Structural Design.

This coefficient for flexible bituminous railway and for flexible pavements depends on the pavement structure, which is characterized by the SN (structural number), an abstract number expressing the strength required for each soils support, given a traffic and serviceability combination. So, for flexible roads, is adopted the value of 6 but in railways a coefficient value of 5 is indicative of the structural rail strength, considering the subgrade support, the service life and layer structure.

The results of the traffic spectrum for the main line considered are shown in Fig. 6.

3.1.4 Railway Traffic Design Life

The design life depends on the railway type and the traffic level, generally, it is longer for the railroads with major traffic to cause the least interference to the exercise due to rehabilitation maintenance works. Generally, the design life is 50 years for the high-speed lines and 30 years for the ordinary lines [40].

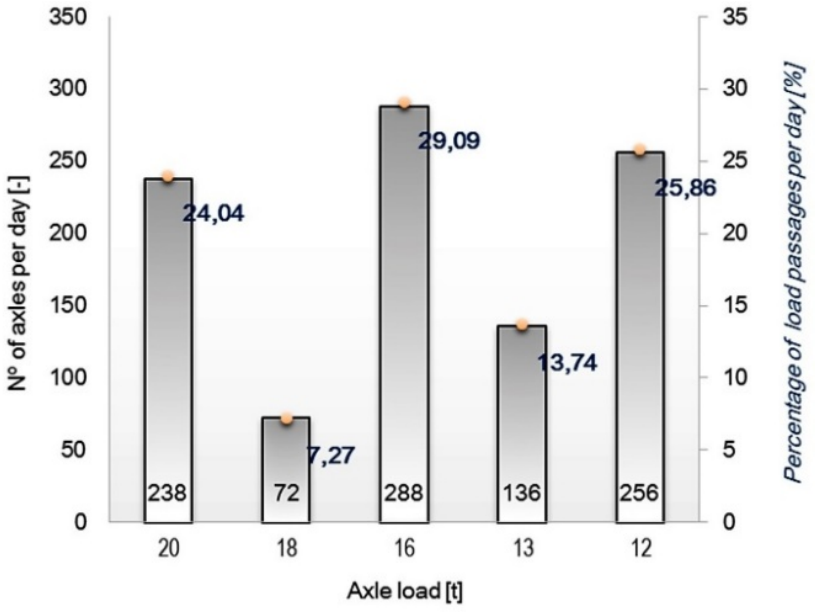

Fig. 6 Traffic spectra of Sicilian main railway line.

The design life is expressed by the number of load repetitions for all the foreseen traffic load combinations and environmental conditions (temperature, moisture, etc). Prediction of structure distresses and maintenance throughout its lifetime can be performed according to the allowable number of load repetitions [40, 41].

Increasing axle loadings result in increased subgrade stresses and asphalt tensile strains increased. The predicted asphalt lives are marginally reduced with increased loadings. The detrimental effects of the higher axle loads can be offset by increasing the effective stiffness of the subgrade.

The traffic level expected over a 30-year period for the three main-lines considered, is summarized in Table 3, adopting a traffic growth rate equal to 0%, 0.2%, 0.4%, 0.6%, 0.8% and 1% (Table 4).

3.1.5 Subgrade Bearing Capacity

The subgrade provides the roadbed upon which all other components of the track structure are placed and has a significant impact on the track's ultimate quality and required maintenance [38].

The loading characteristics of the track dictate the required quality of subgrade. These include the type of transport (freight or passenger), train speed, axle loads, train configuration, wheel condition, tie spacing, and rail condition.

In the layered system, the subgrade is assumed infinite in the vertical downward and horizontal directions. The other layers are assumed finite in thickness but infinite in areal extent. Full continuity is assumed at each interface between the layers. The mechanical behavior of the subgrade depends on:

- geological nature and its elastic properties;
- susceptibility to water;
- levels of stress transmitted;
- the duration and the speed of the loads;
- the number of repetitions of each load.

Although the layer system is assumed to be infinite in areal extent, while the asphalt material is of limited width, this assumption should not affect the accuracy of the results if the rail load is applied more than 0.9 m from the edge. Strength and deformation properties are both important in measuring subgrade performance. The distinction between strength and stiffness is important to understand in railroad subgrade design.

Bearing capacity is the general indicator of strength, while elastic deformation per applied load intensity is represented by the soil modulus. It should also be noted that the stratification of the subgrade may also affect track performance [42].

3.1.6 Analysis of Thermal Contribution

Due to the existence of ballast aggregates for underlayment, the hot mix asphalt and subgrade in railroad trackbed are better protected from environmental effects as compared to highway pavements. The most important effect is the temperature of bituminous sub-ballast, which affects its elastic modulus.

The simulations with KENPAVE and KENTRACK have been fixed to two air temperatures, which represent the average effective temperatures according to the calculation of the Barber Eq. (5), with the minimum temperature being 0 ºC and the highest temperature considered 35 ºC, respectively:

Table 4 Summary of the traffic levels expected.

*RESAL*s at the end of the service life (30 years)			
Traffic growth (%)	Palermo Messina	Catania Messina	Siracusa Catania
0	3.171E+07	1.796E+07	3.131E+06
0.2	3.265E+07	1.849E+07	3.223E+06
0.4	3.362E+07	1.904E+07	3.319E+06
0.6	3.463E+07	1.961E+07	3.419E+06
0.8	3.568E+07	2.020E+07	3.523E+06
1	**3.677E+07**	2.082E+07	3.630E+06

$$T_{pav(z,t)} = T_M + R + (\frac{T_V}{2} + 3R) \cdot F \cdot e^{-Cx} \cdot \sin\left(0.262t - Cx - arctg\left(\frac{C}{hc/K + C}\right)\right) \quad (5)$$

where:

$T_{pav(z,t)}$ = pavement temperature at the depth z and time t (°C);

T_M = mean effective air temperature (0-35 °C);

T_V = maximum variation in temperature (10.5 °C);

$R = 2/3 \cdot (b \cdot I)/24h_c$ = contribution of the solar radiation (8.35 °C);

$h_c = 4.882 \cdot (1.3 + 0.4332 \cdot v^{3/4})$ = surface coefficient depending on the wind speed (24.25 kcal/hours·m^2·°C);

v = wind speed (17.25 km/h);

I = average radiation (5,398 kcal/m^{2}day);

b = absorptivity of surface to solar radiation (0.21*);

C = (0.131·s·w)/K (6.71 hour$^{0.5}$/m);

s = specific heat (0.21 kcal/kg°C);

w = density (2,500 kg/m^3);

K = thermal conductivity (1.5 kcal/m·h·°C); and

x = depth (0.47 m).

* means values of absorptivity in the case of railway sub-ballast, equal to 0.21 [25], and 0.9 [12].

3.1.7 Mechanical Properties

Sub-ballast and subgrade are considered as linear elastic materials. The bedrock is assumed incompressible with a Poisson's ratio of 0.5. Ballast in a newly constructed trackbed behaves non-linearly while in an aged trackbed, it behaves linearly due to being well compacted.

In the asphalt layer, the tensile strain at the bottom of the asphalt layer controls its service life. The design method presented for the standard case study was used under various conditions of traffic, subgrade and climate (Table 5).

The value adopted for the bituminous Poisson ratio (v = 0.4) is the same value used by Rose et al. [43] when validating substructure computer model stress values through in-situ measurements.

Viscosity temperature susceptibility method is used to estimate viscosity of different asphalt binders/cements. The Witczak-E* predictive model for asphalt was specifically incorporated in the updated version. The modulus increases using the new E* predictive model, thus asphalt becomes stiffer, leading to the decreases in asphalt tensile strains and increases in predicted service lives.

To accurately model the asphalt, different temperatures should be used for the different periods since the dynamic modulus is dependent on the temperature. Afterwards, it was possible to calculate the mechanical characteristics of the bituminous materials with the Witczak predictive model [44] based on the volumetric properties of the mixture and the binder characteristics (Eq. (6)).

$$\log|E^*| = -1.249937 + 0.02923\rho_{200} - 0.00167\rho_{200}^2 - 0.002841\rho_4 - 0.058097V_a - 0.802208\,V_{beff}/(V_{beff} + V_a) + \frac{3.971977 - 0.0021\rho_4 + 0.003958\rho_{38} - 0.000017\rho_{38}^2 + 0.00547\rho_{34}}{1 + e^{(-0{,}6033 - 0{,}3133\log(f) - 0{,}3935\log(\mu)}} \quad (6)$$

where:

$|E^*|$ = asphalt mix dynamic modulus (10^5 psi);

ρ_{200} = % material passing to the sieve 0.075 mm;

ρ_4 = % material retained to the sieve 4.75 mm;

ρ_{38} = % material retained to the 9.5 mm sieve;

ρ_{34} = % material retained to the 19 mm sieve;

V_{beff} = effective binder content (% by volume);

Table 5 Standard layer properties for default case.

Railway track	Layer (mm)	Thickness (inch)	Poisson's ratio	Young's modulus (psi) (× 6.89 kN/m^2)
Concrete tie	210	8.27"	0.3	4,000,000
Ballast	350	13.78"	0.2	18,490
Sub-ballast	120	4.72"	0.4	1,305,000
Subgrade	300	11.81"	0.4	21,350
Bedrock	-	-	0.5	10,000,000,000

V_a = air voids (4% by volume);

f = load frequency (28 Hz);

b = percentage of binder (5.5%); and

μ = binder viscosity (10^6 poise).

The complex modulus has been identified as a main parameter for calculating the response of a bituminous structure to traffic loading as well as its resistance to rutting and fatigue [45].

Properties of asphalt binders and mixes are incorporated into Wictzak predictive E^* model to determine asphalt dynamic moduli as an integral step in model evaluation and validation [46]. It is noteworthy that variables related to aggregate gradation (ρ_{200}, ρ_4, ρ_{38}, ρ_{34}), mix volumetric (volume of air voids, V_a, and volume of effective bitumen, V_{beff}) have the most influence on the E^* stiffness of asphalt mixes.

Table 6 shows the temperatures, Poisson's coefficient and modulus of elasticity of each layer of bituminous material at the two frequencies representative of 0 ° C and 35 ° C. These values are obtained through the simulations with Kenpave and Kentrack.

3.2 Temperature Validation Results

The thermal regime within the pavement is governed by the physical, chemical and thermal properties of the layer materials, as these affect the process of propagation of the temperature in the sub-ballast and the substrate. The operating methodology to calculate the temperature gradients is composed of different stages:

- Acquisition from the last 30-years of meteorological temperature values (operated by Sicilian and meteorological Information Service, SIAS (Servizio Informativo Agrometeorologico Siciliano));
- Meteorological data processing, dividing the year and calculating the average max/min temperatures $T^a_{max/min}$ for each year-period;
- Calculate the average air temperature $T_{a(p)}$ of the seasonal periods;
- Temperature inside each layer, in function of the relative average air temperature for each period, using Barber equation.

Certain limitations are solved such as the fluctuations in temperatures that can significantly affect the layer stability, or the different conductivity of the materials. Each simulation for different temperatures (0, 10, 20, 30, 35 and 40 ºC), has considered that in the case of roads and rail, the depth of interest is 31 cm and 47 cm, respectively. Table 7 show the results of temperatures by Barber-Crispino models.

The results after comparison between railway sub-ballast bottom layer and road base bottom layer are represented in Fig. 7.

Table 6 Main parameters for road and railway layers.

Air temperature 0 °C						
		Layer T^a (°C)	η (10^6 poise)	log(E^*)	$\|E^*\|$ (MPa)	v
	WC	8.30	11.6057	1.174	10,282.6	0.4
Road	BC	8.30	11.6057	1.208	11,135.2	0.4
	BA	8.30	11.6057	1.283	13,219.8	0.4
Rail	SB	1.94	59.5026	1.434	18,929.8	0.4
Air temperature 35 °C						
		Layer T^a (°C)	η (10^6 poise)	log(E^*)	$\|E^*\|$ (MPa)	v
	WC	43.3	0.0014	-0.130	510.39	0.4
Road	BC	43.3	0.0014	-0.098	549.56	0.4
	BA	43.3	0.0014	-0.045	621.17	0.4
Rail	SB	36.9	0.0074	-0.235	1,185.68	0.4

(*) WC: wearing course; BC: binder course; BA: base course; SB: sub-ballast layer.

Table 7 Results $T^{a}_{pav(z,t)}$ obtained for road base and railway sub-ballast layers.

Air T^{a}	0 ºC		10 ºC		20 ºC		30 ºC		35 ºC		40 ºC	
No. of hour	Road	Railway	Road	Railway	Road	Railway	Road	Railway	Road	Railway	Road	Railway
0	6.68	2.04	16.68	12.04	26.68	22.04	36.68	32.04	41.68	37.04	46.68	42.04
1	6.26	1.96	16.26	11.96	26.26	21.96	36.26	31.96	41.26	36.96	46.26	41.96
2	5.99	1.88	15.99	11.88	25.99	21.88	35.99	31.88	40.99	36.88	45.99	41.88
3	5.87	1.80	15.87	11.80	25.87	21.80	35.87	31.80	40.87	36.80	45.87	41.80
4	5.93	1.73	15.93	11.73	25.93	21.73	35.93	31.73	40.93	36.73	45.93	41.73
5	6.15	1.68	16.15	11.68	26.15	21.68	36.15	31.68	41.15	36.68	46.15	41.68
6	6.52	1.64	16.52	11.64	26.52	21.64	36.52	31.64	41.52	36.64	46.52	41.64
7	7.02	1.63	17.02	11.63	27.02	21.63	37.02	31.63	42.02	36.63	47.02	41.63
8	7.60	1.64	17.60	11.64	27.60	21.64	37.60	31.64	42.60	36.64	47.60	41.64
9	8.24	1.66	18.24	11.66	28.24	21.66	38.24	31.66	43.24	36.66	48.24	41.66
10	8.89	1.71	18.89	11.71	28.89	21.71	38.89	31.71	43.89	36.71	48.89	41.71
11	9.49	1.78	19.49	11.78	29.49	21.78	39.49	31.78	44.49	36.78	49.49	41.78
12	10.02	1.85	20.02	11.85	30.02	21.85	40.02	31.85	45.02	36.85	50.02	41.85
13	10.44	1.94	20.44	11.94	30.44	21.94	40.44	31.94	45.44	36.94	50.44	41.94
14	10.71	2.02	20.71	12.02	30.71	22.02	40.71	32.02	45.71	37.02	50.71	42.02
15	10.82	2.10	20.82	12.10	30.82	22.10	40.82	32.10	45.82	37.10	50.82	42.10
16	10.76	2.17	20.76	12.17	30.76	22.17	40.76	32.17	45.76	37.17	50.76	42.17
17	10.54	2.22	20.54	12.22	30.54	22.22	40.54	32.22	45.54	37.22	50.54	42.22
18	10.17	2.25	20.17	12.25	30.17	22.25	40.17	32.25	45.17	37.25	50.17	42.25
19	9.67	2.27	19.67	12.27	29.67	22.27	39.67	32.27	44.67	37.27	49.67	42.27
20	9.08	2.26	19.08	12.26	29.08	22.26	39.08	32.26	44.08	37.26	49.08	42.26
21	8.45	2.23	18.45	12.23	28.45	22.23	38.45	32.23	43.45	37.23	48.45	42.23
22	7.80	2.18	17.80	12.18	27.80	22.18	37.80	32.18	42.80	37.18	47.80	42.18
23	7.20	2.12	17.20	12.12	27.20	22.12	37.20	32.12	42.20	37.12	47.20	42.12
Δ	8.35	1.95	18.35	11.95	28.35	21.95	38.35	31.95	43.35	36.95	48.35	41.95

Note: Road base layer depth = 31.5 cm; Sub-ballast railway depth = 47 cm; Values of absorptivity in the case of railway = 0.21 [25] and of road = 0.9 [12].

The experimentation conducted has allowed the determination of the temperatures in the sub-ballast layer of asphalt mixture. The variation of temperatures during the year is found to be approximated by a sinusoidal function. It has been found that the speed and depth have a positive effect on the pavement temperature predictions, the maximum daily pavement temperature increases by increasing the wind speed and depth.

Air temperature and solar radiation were found to have the highest positive impact, and pavement temperature fluctuations follow a sine curve with a period of one day. Based on the acquired measurements, we determined the average seasonal temperatures in the layer, for the spring, summer, autumn and winter, respectively, related to Sicilian climatic conditions.

The following graph shows the evolution of the temperature in each layer for the most representative air temperatures (0 ºC and 35 ºC) in each section of pavement and railway, along a sinusoidal cycle marked by the daily hours (Fig. 8).

4. Problem Statement 02

4.1 Superpave Mix-Design for Railways

SGC (Superpave volumetric mix design) is the key step in developing a well-performing asphalt mixture [47]. It was developed as the optimal laboratory tool that more closely simulates field compaction of asphalt mixtures. The SGC is a 1.25º fixed angle, 600 kPa

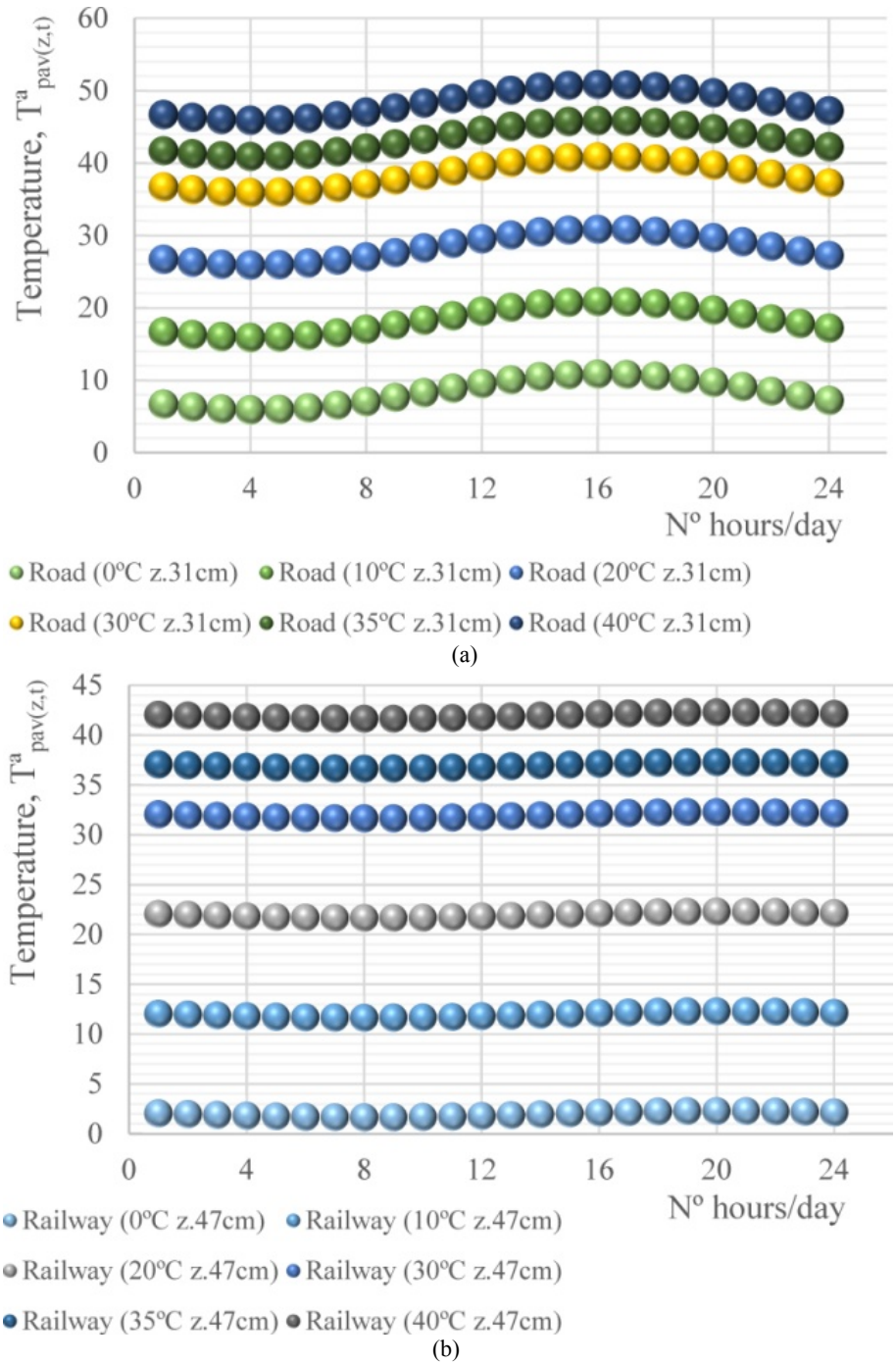

Fig. 7 Daily variation of T^a in the pavement at the depth z and time t (°C) between: (a) road and (b) railways.

pressure and rate of gyration (30 rev/min) compactor that creates samples 150 × 120 mm in diameter × target height. The compacted samples are measured for specific gravity and the volumetric properties are calculated. The SGC also provides the ability to investigate the aggregates properties at void levels representing construction throughout its intended life cycle.

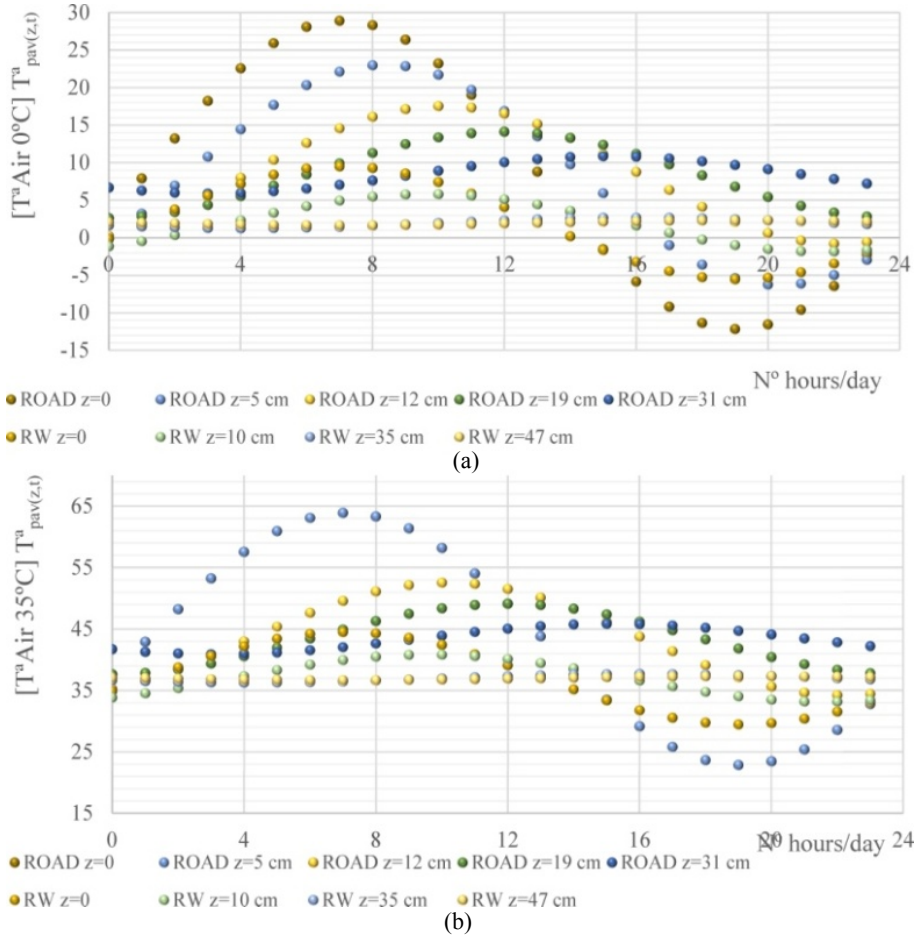

Fig. 8 24 hour-T^a variation in the pavement at different depths (air T^a 0°C-35ºC) between: (a) road and (b) railways.

As the traffic level for the designed rail track increases, the design requirements increase to improve reliability. At the higher traffic levels, extensive performance testing is recommended to assure the highest reliability. A unique feature of the Superpave system is that its tests are performed at temperatures and aging conditions that more realistically represent those encountered by in-service sub-ballasts.

The following case study describes the use of a Superpave performance model to support the fatigue racking distress in railway section, considering the environmental parameters and performance prediction model established.

In recent years, several research efforts have been employed to investigate and refine the Superpave mix design system of HMA for new construction [48].

In predicting performance for multilayer, specific ground rules govern the treatment of the main layer distresses: permanent deformation, fatigue and low-temperature cracking. Superpave allows to identify the input for the material properties for each layer below the asphalt layer, and would be extended to the prediction of fatigue cracking as main distress.

The values established in the original regulations of Superpave contemplated diverse levels of gyration, that represent seven traffic levels for each of four climates. In the years following the improved N_{design} value, the climatic region factors were eliminated and incorporated in the bitumen selection process depending on the PG (performance grade).

Table 8 shows the recent compaction parameters to be set up when using Superpave gyratory compactor [49]. The number of gyrations is selected based on the traffic level calculated.

A relationship has been established between the number of maximum *RESAL*s determined for the rail

Table 8 Parameters for gyratory compactor.

*ESAL*s (10^6)	$N_{initial}$	N_{design}	N_{max}
< 0.3	6	50	75
0.3 to < 3	7	75	115
3 to < 30	8	100	160
≥ 30	9	125	205

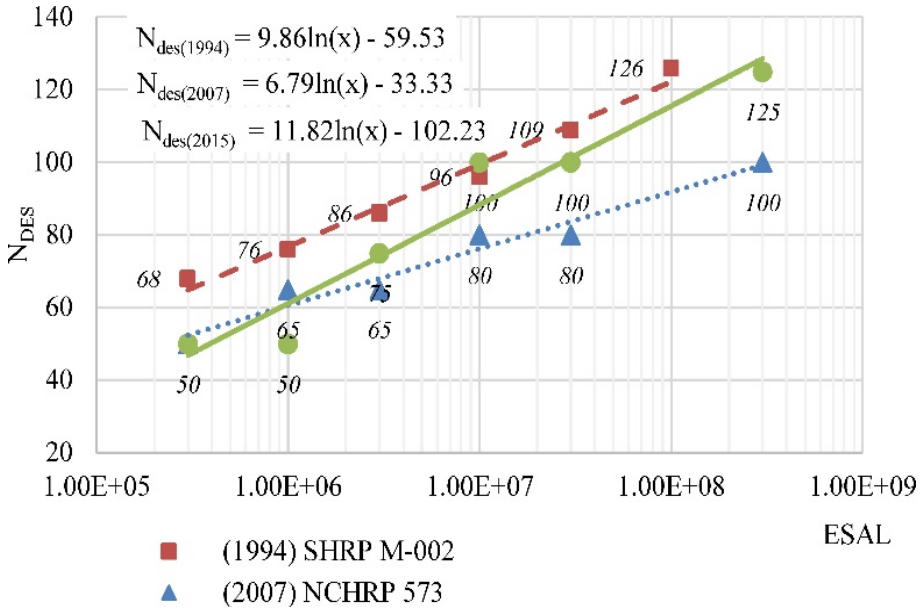

Fig. 9 N_{design} recommended by Superpave standards.

sub-ballast of the study case, and the values that in recent years have been determined for the Superpave. In summary, diverse regression curves are applied corresponding to the values of the standards and codes (Fig. 9):

- (1994) SHRP A-407 / M-002;
- (2007) NCHRP Report 573;
- (2015) AASHTO R35.

Subsequently, it is considered the most recent.

Kentrack@ considered the recent asphalt grading trackbed system and their properties inside the software. For the past years, trackbed construction has used the Superpave PG system based asphalt binders. Therefore, the program maintains the previous asphalt grading system and incorporates information of the new asphalt grading system for comparison purposes [47]. In this study, the recent updates of Superpave values were applied. Once the traffic spectrum was converted in *RESAL*, it was calculated the N_{design}.

Therefore, considering the logarithmic regression from the interpolation of the values of *ESAL*-N_{des} [49], it has been determined a correspondence between the R_{ESAL}s and number of gyrations (Fig. 10).

Using the values as shown in Table 4, the N_{design} for the bituminous sub-ballast was calculated with each value of *RESAL*s. The traffic growth rate was selected equal to 1%. Thus, based on the results N_{design} for the Sicilian traffic (see Table 3) and temperatures, the energetic parameter for compaction is equal to 100 cycles.

A correspondence between the number of compact-gyrations and the rail axle load value found, has been defined as is shown in Fig. 11 for the three track lines studied (Palermo-Messina, Catania-Messina, and Siracusa-Catania).

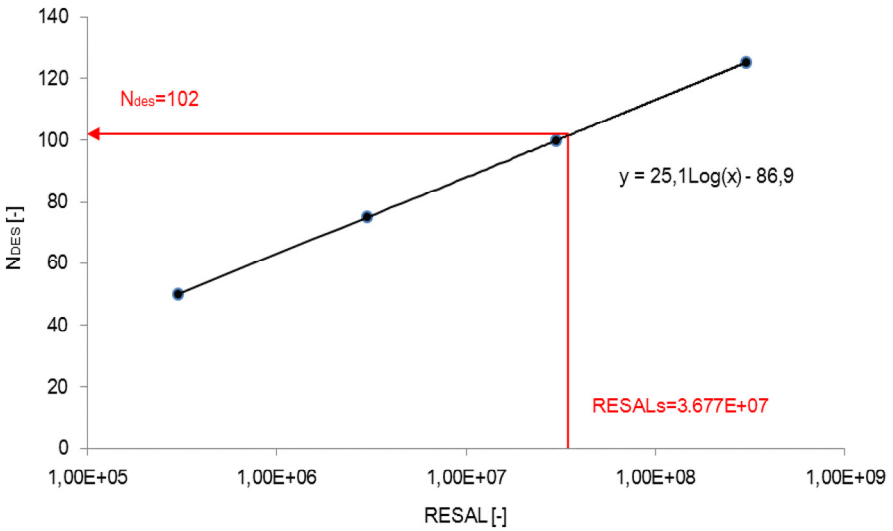

Fig. 10 Logarithmic regression by interpolation of N_{des} values.

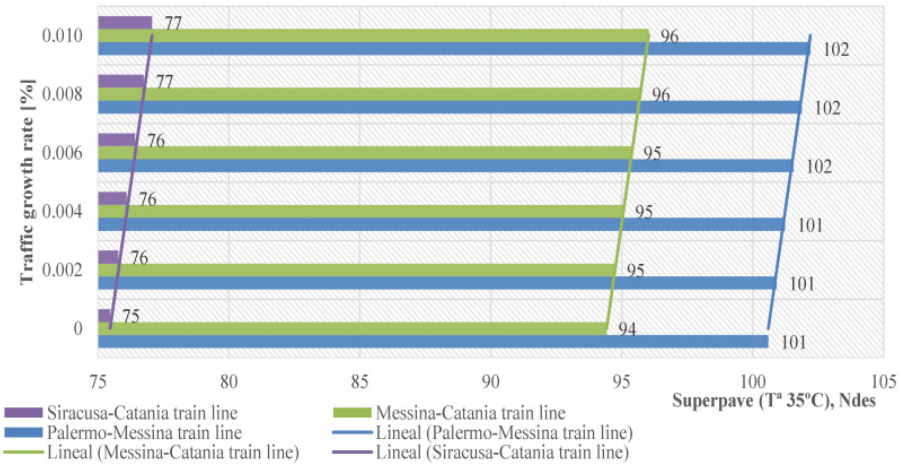

Fig. 11 N_{design} obtained for different track-lines and different values of annual traffic growth rate.

5. Experimental Results & Design

5.1 Materials and Mixture Design

During these study, different mixes were characterized by volumetric mix-design, obtaining optimal mixes with diverse amounts of asphalt binders (4%, 5%, 5.5%, 6%, 6.5% and 7% of total binder weight), and diverse quantity of rubber proportion (0%, 1.5%, 2% and 3% of the total weight of the aggregates in volumetric substitution) was studied. The mixture design was developed and performed at the Laboratory of Materials and Civil Engineering of the University of Palermo (Italy).

Using these amount of binders, six different bituminous mixtures (1 HMA_{RFI} b.4%, 1 DRY 1.5% b.5%, 1 DRY 1.5% b.5.5%, 1 DRY 2% b.6%, 1 DRY 2% b.6.5%, 1 DRY 3% b.7% mixtures) were manufactured to assess the influence of the rubber on the performance of the rubberized asphalt materials by dry process for a bituminous sub-ballast layer. The reference mixture is a conventional hot mix asphalt without rubber as dense graded mixture with a limestone nature of aggregates, with a 4% of a conventional bitumen B50/70 in accord with satisfactory previous studies.

The manufacturing process with the rubber involved

a protocol in order to better homogenize the aggregates with rubber by dry technology and enhance the digestion process, to provide final cohesion and optimal compaction.

The specifications for the bituminous sub-ballast are defined by the RFI (Italian standard). This standard is based on the results of the Marshall and water sensitivity tests, and it specifies a minimum void content between 3%-5%. Through selection and prior testing of the inert material, the individual fractions of aggregates were combined in precise percentages individually, to produce asphalt mixtures, which exhibit adequate levels of inert interlaced material (Table 9).

These mixtures were optimized in laboratory after testing different binder's content to relate the compaction and volumetric characteristics with changes in the coarse-fine gradations and the corresponding ratios of filler-aggregates.

The DP (dust proportion) was measured as a parameter that affects the mix properties. An excessive dust dries out the mix reducing asphalt film thickness and durability. DP is determined as the ratio between $P_{0.075}$, the aggregate content passing the 0.075 mm (75 μm) sieve, and P_{be}, effective asphalt binder content, both as percent by mass of aggregate, to the nearest 0.1%. For each mixture, the values of DP were between 0.7 to 1.4, within the acceptable values required for optimum durability for sub-ballast.

The mixtures for the characterization of air voids, the dust-to-asphalt ratio, the study of aggregate voids, VFA (voids filled of asphalt) and VMA (voids in the mineral aggregate) percentages, were performed until satisfactory results (Table 10).

When the binder and aggregates have been selected for the asphalt mixture, they must be combined to produce the optimum mixture properties.

The SGC is used to determine the optimum mixture. Once the overall procedure for the Superpave mix design calculation was defined, a laboratory verification was conducted. The methodology was applied to determine the number of gyrations in the specific case of the track line connecting Messina and Catania, with a traffic growth rate selected equal to 1%. The specifications for the bituminous sub-ballast are defined by the (RFI).

The Superpave mix design system contains specific performance related characteristics in selecting acceptable aggregate materials (washed sieve analysis of all fractions, mineral dust filler, control points, Fuller's curve (n = 0.45)…).

In this research, the grading curve has been optimized to lower levels within the limits established by the Italian sub-ballast standard (RFI), as is shown in Fig. 12.

Table 9 Granulometric distribution of aggregates.

Target		HMA	DRY1.5	DRY2.0	DRY3.0
Sieves (mm)		% passing			
31.5	100.00	100.0	100.0	100.0	100.0
22.4	92.86	92.39	92.26	92.22	92.11
16	76.75	77.18	76.82	76.70	76.45
11.2	63.97	63.28	62.77	62.60	62.32
8	54.41	54.96	54.23	53.98	53.38
5.6	46.36	47.20	46.32	46.02	45.32
4	41.00	38.40	37.72	37.49	37.41
2	27.25	27.75	27.45	27.35	27.62
1	18.23	20.69	20.61	20.59	20.79
0.40	12.69	15.72	15.80	15.82	15.98
0.177	9.28	10.41	10.51	10.54	10.65
0.063	6.75	6.76	6.85	6.88	6.94

(*) Granulometric grading curve based on target values from sub-ballast mixtures [39].

Table 10 Percentage of each fraction crude for constitution of the theoretical recipes.

Type of fraction	Filler	Sand	Ø5-10 mm	Ø10-15 mm	Ø20-25 mm	Ø25-30 mm	Σ
Mixtures	< 0.063	1-4	5-8	8-11.2	11-22.4	< 31.5	
RFI_HMA (ρ_{mix}, g/cm^3)	12.24%	24.60%	5.21%	18.29%	18.49%	21.16%	100%
	2.748	-	-	-	-	ρ_{aggr}	2.809
DRY1.5% (ρ_{mix}, g/cm^3)	12.45%	23.79%	4.62%	18.98%	18.65%	21.52%	100%
	2.716	-	-	-	-	ρ_{aggr}	2.808
DRY2% (ρ_{mix}, g/cm^3)	12.52%	23.51%	4.42%	19.21%	18.70%	21.65%	100%
	2.700	-	-	-	-	ρ_{aggr}	2.808
DRY3% (ρ_{mix}, g/cm^3)	12.66%	22.94%	4.01%	19.69%	18.80%	21.90%	100%
	2.687	-	-	-	-	ρ_{aggr}	2.808

Mix design			
Rubber substitution (% of total mix by)			
Mixture	Asphalt (%)	Weight (%)	Volume (%)
DRY 1.5	5.5	1.5	3.02
	6.0	1.5	2.98
DRY 2.0	6.0	2.0	3.95
	6.5	2.0	3.90
DRY 3.0	7.0	3.0	5.71

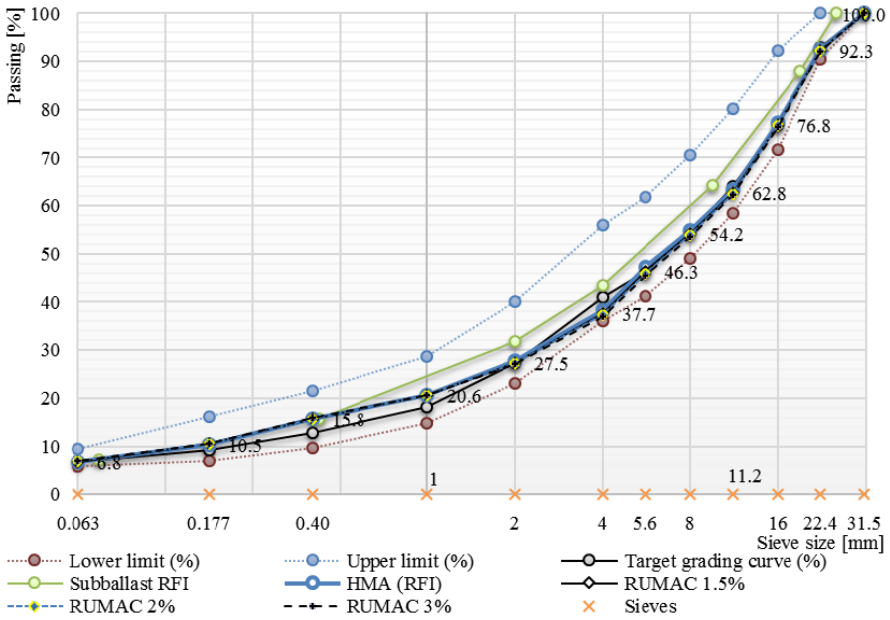

Fig. 12 Target grading curve of the bituminous sub-ballast.

Thus, the procedure used for the mix-design of the mixtures was in accord with the Superpave but adopting the Italian standard, which is based on the results of the Marshall and water sensitivity tests, and it specifies a void content of 4%-6%, a Marshall stability of 10 kN, and a higher indirect tensile strength at 15 ºC of 0.6 N/mm^2.

The mixture will be placed at a depth of 47 cm from the surface of the rail-track (see Fig. 2). The next step is selection of the asphalt binder for specification compliance, so following RFI standard, a bituminous binder must be type 50/70.

The content of bitumen based on the total mass of the aggregates will have to correspond to the optimum content obtained in the laboratory, with a tolerance of ± 0.5%.The characteristics of the materials used for the

fabrication of the bituminous sub-ballast are summarized in Table 11.

The crumb rubber used in this case by dry process had two particle sizes of 0.2-4 mm and 2-4 mm (Fig. 13).The rubber aggregate with gap-gradation is a two-component system in which the fine gradation is believed to interact with the asphalt cement while the coarse rubber performs as an elastic aggregate in the hot mix asphalt mixtures [50].

Each mixture has a different proportion of rubber to be representative of the industry conditions, and to ensure the equal distribution during the rubber-bitumen reaction. It should be underlined that the mineral skeletons of the mixes were the same and that the mixes differed in the components proportion, the type and content of binder, with this fact, the comparison of results and the optimization is facilitated. Its properties are shown in Table 12.

Table 11 Characteristics of the materials used for the bituminous sub-ballast production.

Bitumen			
Properties		Standard	Value
Penetration at 25 °C		EN1426:2007	53
Penetration index (-)		EN12591 Annex A	-0.575
Softening point (°C)		EN1427:2007	50
Bulk gravity (g/cm^3)		EN 15326:2007	1.033
Viscosity at 150ºC (Pa·s)		ASTM D2493M-09	0.195
Equiviscosity values by	0.28 Pas	EN 12695:2000	143.1
Brookfield viscosity (°C)	0.17 Pas	AASHTO T316-04	156.2
Aggregates (limestone)			
Properties		Standard	Value
Los Angeles abrasion loss (%)		EN 1097-2:2010	20.8
Bulk spec. gravity aggregates (g/cm^3)		EN 1097-3:1998	2.82
Bulk specific gravity sand (g/cm^3)		EN1097-6:2013	2.84
Bulk specific gravity filler (g/cm^3)		EN1097-7:2009	2.70
Resistance to fragmentation		EN1097-2 (%)	20.83
Determination of particle shape		EN933-3 (%)	10
Sand equivalent (> 45) (%)		EN933-8	61
Total sulphur content (< 0.5) (%)		EN1744-1	0

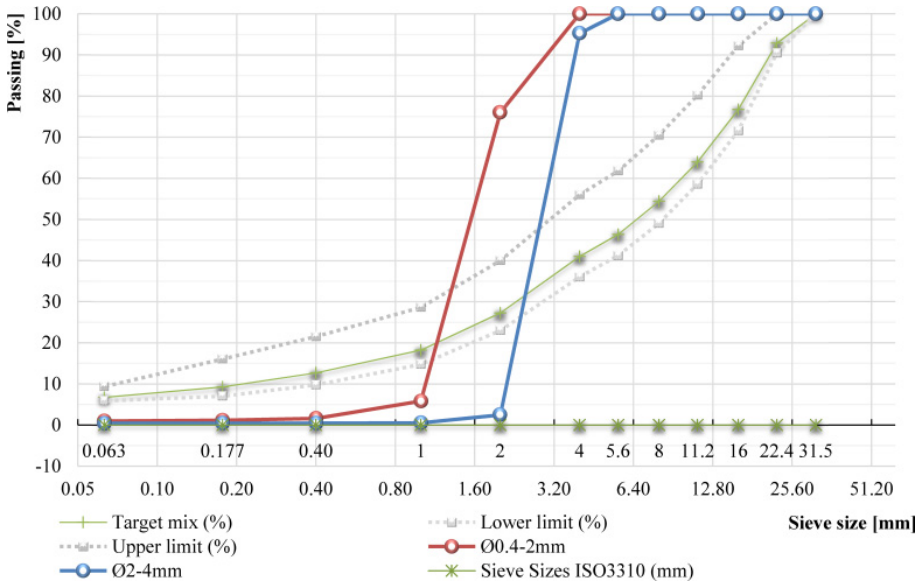

Fig. 13 Rubber sieve analysis (grading curves Ø2-4 mm; Ø0.4-2 mm).

Superpave mix-design of the bituminous sub-ballast was carried out, setting the N_{design} equal to 102 (based on the design high air temperature of the paving location, 35 ºC, annual traffic growth rate, 1%, and level of >107 *ESAL*s) for a conventional hot mix asphalt without rubber.

For mixtures with rubber, according to the methodology reflected, the number of volumetric gyrations is increased, to compensate the rebound and relaxation effect of the rubberized mixture after post-compaction, due to the energy accumulated during the compaction, thus avoiding the effect of extension of the mixture during the period of post-compaction.

In this way, the percentage of target voids, the apparent density and the protection of a possible deterioration of the internal structure is maintained. In this case, the values adopted are shown in Table 13.

5.2 Results

The reference mix in this study was a bituminous dense graded mixture for sub-ballast layers according to RFI [39]. This is a hot mix asphalt with a maximum size of 31.5 mm coarse aggregate. Limestone for the fine fraction and a 6.75% amount of filler passing sieve 63 μm. Of this filler, 72% had a particle size smaller than 0.177mm. To guarantee good adhesion and chemical bonding, the mixtures were designed with a fine fraction less than 2 mm.

The manufacturing temperature for a conventional B50/70 bitumen was 160 ºC and the compaction temperature was set at 145 °C, which were carried out with the Brookfield viscometer, according to the viscosity values [51]. The higher temperature thus guaranteed the workability of the mix.

Table 12 Properties of the rubber added to the dry-process CRM mixes.

Color	Black
Particle morphology	Irregular, undisclosed
Moisture content (%)	< 0.75
Textile content (%)	< 0.65
Metal content (%)	< 0.10
Maximum density according to proportion 60% Ø0.4-2 mm; 40% Ø2-4 mm)	
Standards: C.N.R. UNI-1 ; ASTM C128 ; UNE 12597-5:2009	
T^a water: 27 ºC (density 1.00025 gr/cm^3)	Pycnometer test
Weight of sample (gr)	500
Weight of pycnometer, *m*1(gr)	767
Weight of pycnometer with sample mass, *m*2 (gr)	1,270
Weight of pycn. +sample ssd+water, *m*3 (gr)	3,106
Weight of pycnometer filled of water, *m*4 (gr)	3,039
Maximum specific gravity of rubber (g/cm$^{3)}$	1.1536

Table 13 Volumetric mix design characteristics.

N_{des}	102	150	180	290
Characteristics of the mixtures	RFI b. 4%	DRY1.5% b. 5.5%	DRY2% b. 6.5%	DRY3% b. 7%
Mixture weight (*)	5,460	5,460	5,460	5,460
Aggregate mass	5,250	5,176	5,127	5,103
SG aggregates	2.809	2.808	2.808	2.808
%Inert part	96.15%	94.79%	93.89%	93.45%
Bitumen mass	210.0	284.5	333.4	357.4
S. gravity binder	1.033	1.033	1.033	1.033
% binder	3.85%	5.21%	6.11%	6.55%
γ_{max} (g/cm^3)	2.634	2.577	2.541	2.524

(*) Optimal inert part for a specimen of Ø150 × 120 mm.

Previously, for the hot mix asphalt mixture as reference mix selected, to obtain the target air voids percentage of 3%, a volumetric mix design procedure was developed with four different bitumen percentages (3.6%; 4.0%; 4.5%; 5.0%) of the total weight of aggregates compacted using the gyratory compactor. Between three and four specimens for each mixture with different percentages of bitumen were fabricated for the determination of the maximum theoretical specific gravity.

Finally, for a binder 4% content, a 2.74% of air voids at N_{design} was achieved as the target value [49] in the case of HMA mixtures. For mixtures with rubber, the percentage of voids varies between 3.01% and 3.37%. Therefore, it is never possible to exceed the maximum value of an established 4% of voids for a suitable bituminous mixture in sub-ballast. The dry-process mixes were manufactured with a digestion time between 60, 90 and 120 min. The digestion time enhances the interaction between binder and rubber modifying the mechanical properties of the mixes.

An important step inside the volumetric compaction by Superpave is the optimal finding of the relationship between mass inert part and height of the final specimen, in that case, cylindrical specimens of Ø150 × 120 mm for gyratory compaction and Ø100 × 65 mm by Marshall compaction were selected.

According to the sub-ballast optimal thickness of layer, as we can see before, a height of 120 mm value corresponds with sub-ballast layer modelized in rail track, so for an optimal compaction, it was needed to find the optimal relation between binder content and inert part amount of aggregates. This process was repeated several times until the designed aggregate structure and the binder content produce specimens with the desired volumetric properties in each case.

An example is shown in Fig. 14 for the HMA mixtures. For this, previous mixtures were made with a

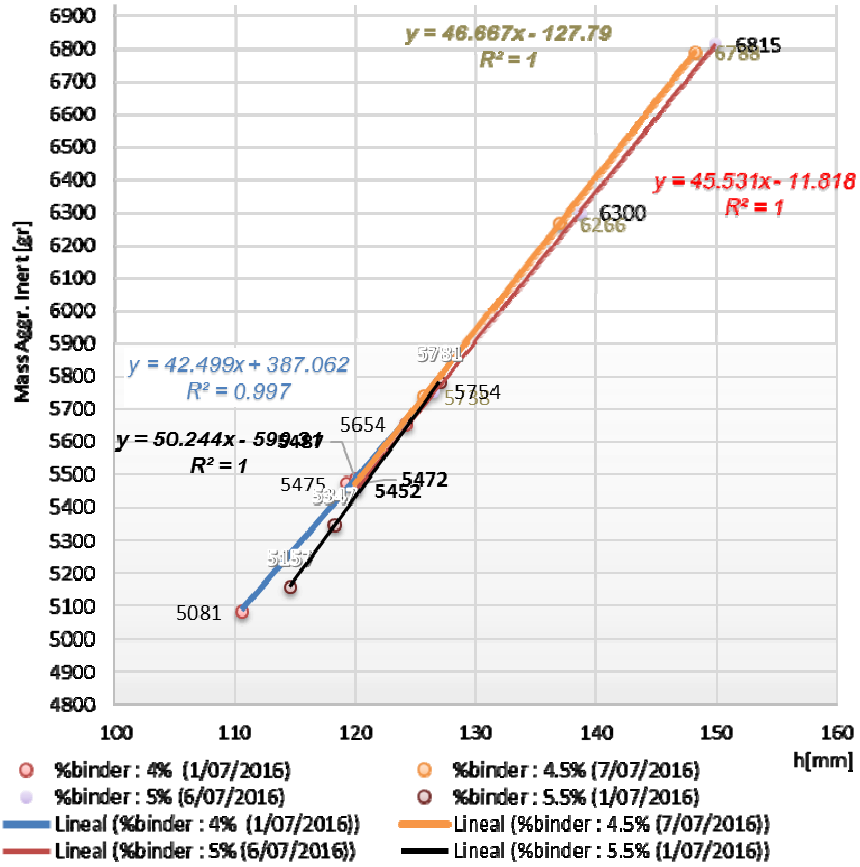

Fig. 14 Relationship between mass inert part and height samples for the reference mixture.

variation of bitumen content that ranged from 4% to 5.5%.

After compacting the specimens to N_{des} gyrations, it has been determined the bulk specific gravity (Γ_{mb}) and the theoretical maximum specific gravity (Γ_{mm}) of each of the four mixtures (EN 12697-6). Comparing the results, the densification curves for each mixture are plotted (Fig. 15).

The number of gyrations used for compaction was, as we have seen, 102 cycles for the HMA reference mixture, 151 cycles for the DRY 1.5% mixture, 181 cycles for the DRY 2% mixture, and 291 cycles for the DRY 3% mixture, based on this new methodology approach showed before, based on design high air temperature of Sicily and the traffic level in R_{ESAL}s.

A densification curve for each mixture are plotted indicating the measured relative density at each number of gyrations (%G_{mm}) versus the logarithm of the number of gyrations. Workability, densification and final air voids content are summarized in the next graphs (Figs. 16 and 17).

To ensure compaction and densification, for each mixture were observed the aggregate interlock, and The air void content around 3%. So, this is reflected in the logarithmic trend equations:

$HMA_{(b.4\%)}$ $\Gamma_{mm}\cdot(N_{des}\cdot 102) = 3.633\ln(x) + 80.954$

$DRY_{1.5/5.0}$ $\Gamma_{mm}\cdot(N_{des}\cdot 152) = 3.426\ln(x) + 80.964$

$DRY_{1.5/5.5}$ $\Gamma_{mm}\cdot(N_{des}\cdot 152) = 3.277\ln(x) + 81.595$

$DRY_{2.0/6.0}$ $\Gamma_{mm}\cdot(N_{des}\cdot 181) = 2.359\ln(x) + 86.209$

$DRY_{2.0/6.5}$ $\Gamma_{mm}\cdot(N_{des}\cdot 181) = 2.306\ln(x) + 86.864$

$DRY_{3.0/7.0}$ $\Gamma_{mm}\cdot(N_{des}\cdot 291) = 1.806\ln(x) + 86.955$

Fig. 16 shows a plot of the gyratory compaction curves of the different N_{des} gyration mixes. The compatibility of these mixes is quite different even though they both meet 3% air voids at 100 gyrations (except dry 3%). One mix is much more sensitive to the gyration level than the other. In one case, changing the gyration level will have much less effect on changes in binder content and VMA.

After compaction, each sample was 24h cooled to room temperature without being removed from the mould with the purpose to avoid the bounce back effect due to the swelling of rubber. Because it was observed a dilatation (expansion) of the specimens after 7 days, final air voids are considered to precise the optimal binder content (Fig. 18 and Table 14).

From the tests conducted, it emerged that the sub-ballast mixture at N_{design} achieved the target voids content with 4% of bitumen in relation to the weight of aggregates, for a conventional mixture without rubber.

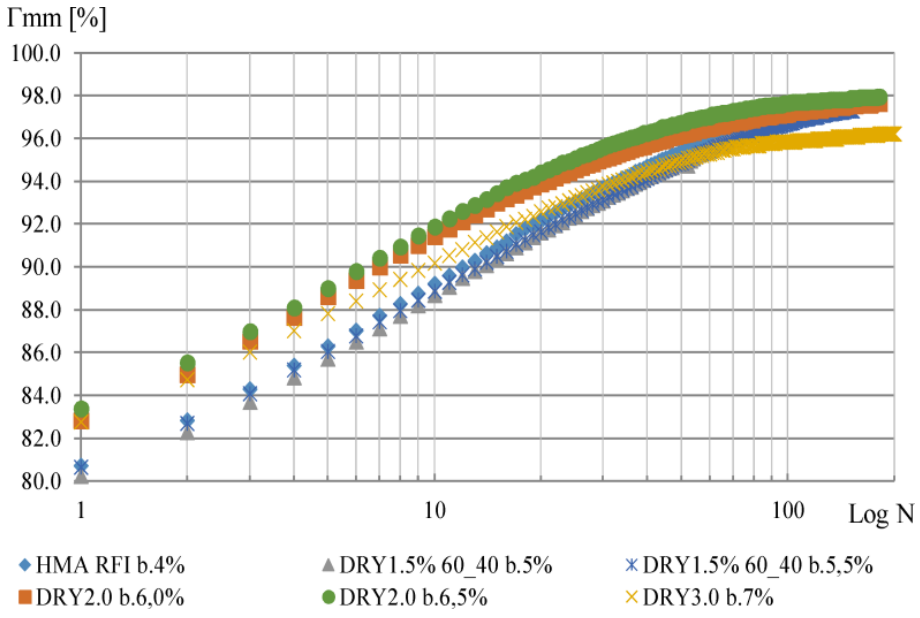

Fig. 15 Comparison between compaction curves.

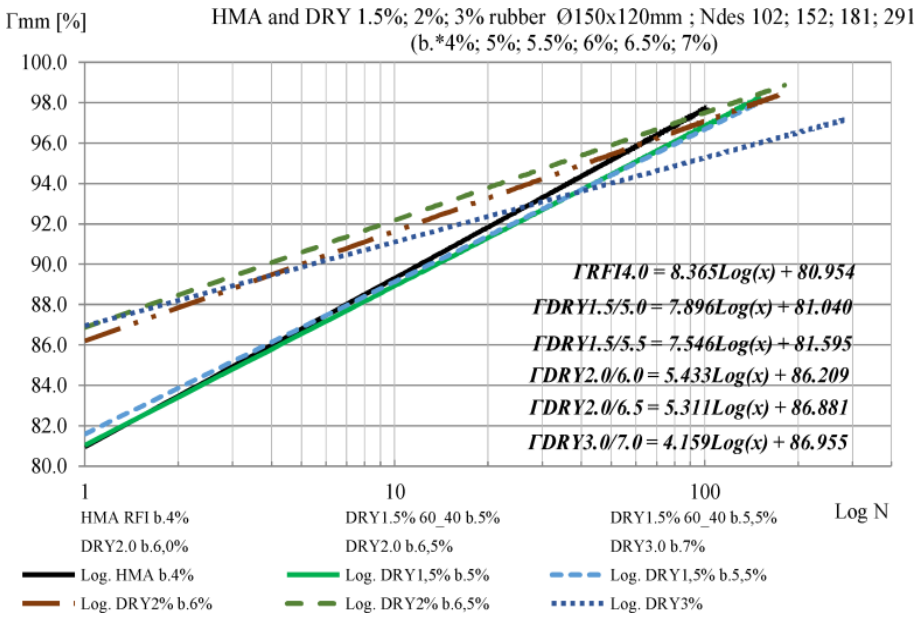

Fig. 16 Trend lines of final compaction curves using Superpave mix-design.

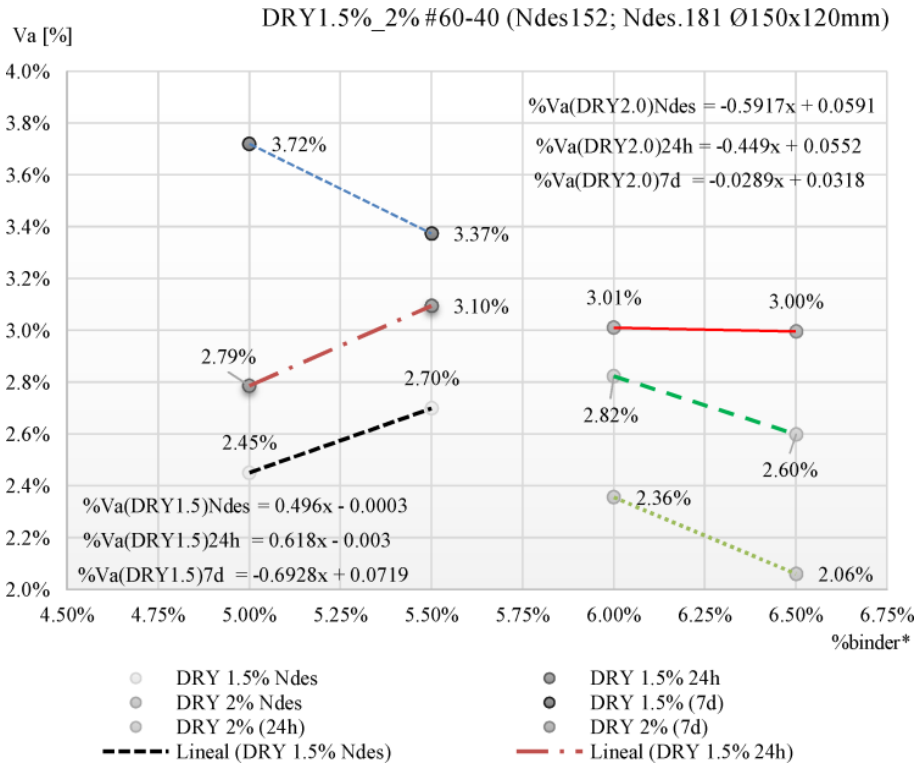

Fig. 17 Mean values of air voids of each mixture. Trend equations to determine the optimal percentage of bitumen.

To ensure capabilities, the target voids content was lowered from 4% of the original SGC to 3% with the consequent increase of bitumen content as reported in Fig. 19.

In the rubberized cases, the optimal binder content and mix design specifications are described in Table 15.

It is the VMA requirement that controls the binder content. The VMA inspects the total voids in the mixture and the air void content (*Va*), and serves as a check between the void content of the mineral part, the percentage of asphalt and the air voids.

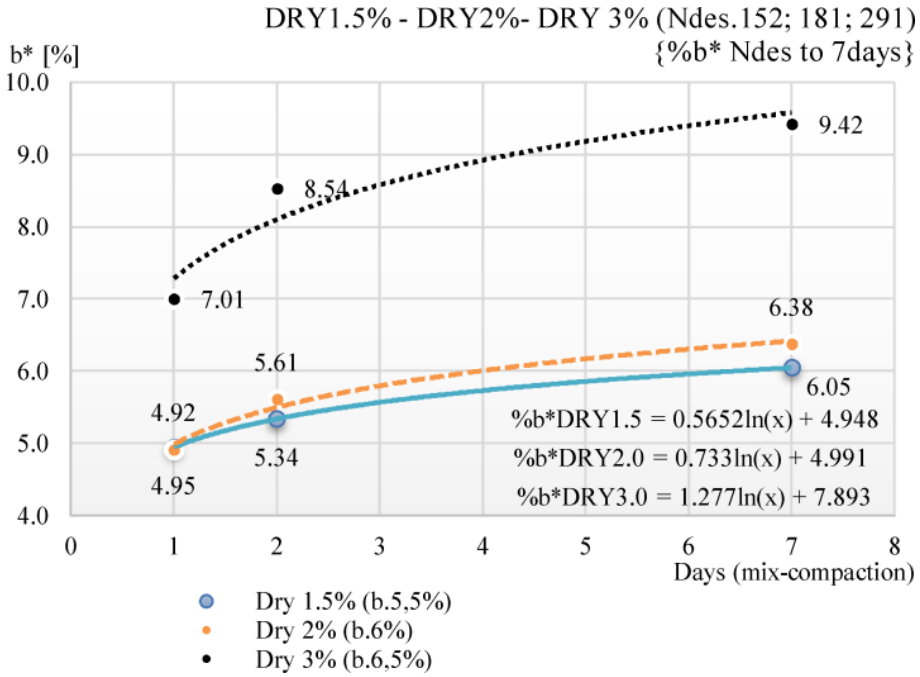

Fig. 18 Optimal binder content after one week due to the swelling effect of rubberized compacted specimens.

Table 14 Optimal binder content for rubberized mixtures to achieve a target value of 3% of air voids by dry process.

Mixture	%Va*	%b*$_{(Ndes)}$	%b*$_{(24h)}$	%b*$_{(7d)}$
Dry 1.5%	3.0%	4.95%	5.34%	6.05%
Dry 2%	3.0%	4.92%	5.61%	6.38%
Dry 3%	3.0%	7.01%	8.54%	9.42%

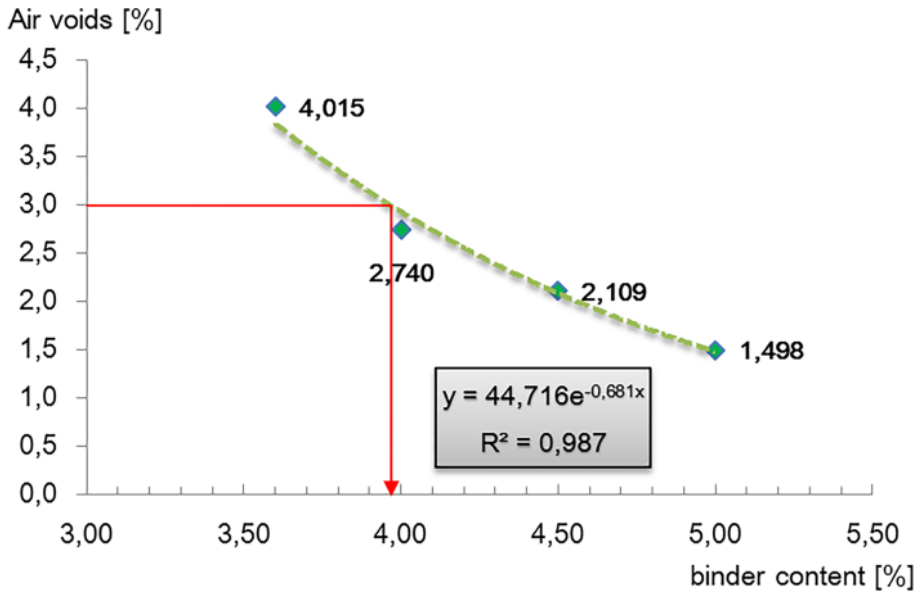

Fig. 19 Plot of percent air voids versus binder content. Optimal bitumen quantity in reference HMA mixture.

Table 15 Volumetric compaction results for each mixture.

Mix(%)	Specimen Ø15×12cm	*H.* N_{des} (mm)	*H.* 24h (mm)	*H.* 7d (mm)	*Va*(%) N_{des}	*Va*(%) 24h	*Va*(%) 7_{days}
RFI	$RFI^{01}{}_{4\%}$	114.30	113.33	113.33	2.78%	2.78%	2.78%
	$RFI^{02}{}_{4\%}$	115.90	115.50	115.50	2.70%	2.70%	2.70%
Dry 1.5%	$DRY^{01}{}_{5.0/1.5}$	121.30	121.99	121.99	2.43%	2.76%	2.78%
	$DRY^{02}{}_{5.0/1.5}$	122.20	123.08	123.08	2.48%	2.81%	4.66%
	$DRY^{03}{}_{5.5/1.5}$	121.70	122.62	122.70	2.39%	2.79%	3.21%
	$DRY^{04}{}_{5.5/1.5}$	121.70	121.74	121.74	3.01%	3.40%	3.54%
Dry 2%	$DRY^{01}{}_{6.0/2.0}$	122.40	122.50	122.60	2.21%	2.67%	2.77%
	$DRY^{02}{}_{6.0/2.0}$	120.40	121.00	122.91	2.51%	2.97%	3.25%
	$DRY^{03}{}_{6.5/2.0}$	120.90	122.00	122.07	1.94%	2.48%	2.96%
	$DRY^{04}{}_{6.5/2.0}$	120.70	121.00	123.10	2.18%	2.72%	3.04%
Dry 3%	$DRY^{02}{}_{7.0/3.0}$	121.90	123.58	123.68	3.50%	4.27%	4.42%
Mix design specifications after post-compaction							
Mix	Dust-to-asphalt ratio, DP	*b* (%)	*VMA* (%)	*VFA* (%)	*Γ*max (g/cm^3)	*Γssd* (g/cm^3)	*Γmm* (%)
RFI	0.892	4.0	12.36	77.86	2.636	2.565	97.26
Dry 1.5%	0.716	5.0	14.95	75.38	2.596	2.508	96.61
	0.709	5.5	15.60	78.37	2.577	2.500	97.02
Dry 2%	0.670	6.0	16.21	81.44	2.559	2.494	96.67
	0.620	6.5	17.11	82.48	2.541	2.479	96.25
Dry 3%	0.590	7.0	18.90	78.38	2.524	2.431	95.68

If the number of gyrations inside the SGC was lower, the result would be a weaker internal matrix-structure, whose aggregate content would be less homogeneous and the void content would be greater. By means of a correct relation between bitumen and total mass to be introduced in each specimen, an optimum distribution of the percentage of voids and the necessary binder content were obtained. Thus, it is shown in Fig. 19 as an example of optimal bitumen quantity in reference mixture.

This could result in a mixture characterized by a low permanent deformation resistance. However, rutting should not represent a concern in the track-bed because of the presence of the ballast, which allows to distribute the pressure of the axle loads over a wide area.

Finally, the effect of extreme air temperatures is minimized by the presence of the upper layers. The specimens, as a valid criterion of orientation, were developed with 120 mm of height after compaction in analogy of the real thickness of the sub-ballast layer, and a Ø150 mm according to the Superpave gyratory compactor, as shown in Fig. 20.

For each specimen prepared, the asphalt binder (135-150 ºC), aggregates (160-190 ºC) and compaction moulds (150 ºC) were heated to the proper mixing temperature according to the mixture type and then were removed and stored at room temperature (20 ºC) after 24h of post-compaction.

During mixing period, rubber swells and the amount of bitumen absorbed increased which causes a stiffer residual bitumen that must be controlled. This fact responds to the need to comply with the following optimum manufacturing protocol (Fig. 21), with the aim of avoiding the absorption effect of the rubber and subsequent structural internal swelling, which leads to deterioration of the specimen.

5.2.1 Moisture Sensitivity

The final step in the Superpave mix-design is to evaluate the moisture sensitivity of the design mixtures by performing AASHTO method of test T283 (resistance of compacted bituminous mixture to moisture induced damage for Superpave) on the design rubber-aggregate structure. One subset of at least three specimens are controlled and subjected to a partial

Fig. 20 Compacted SGC specimens of HMA_RFI 15 × 12 cm.

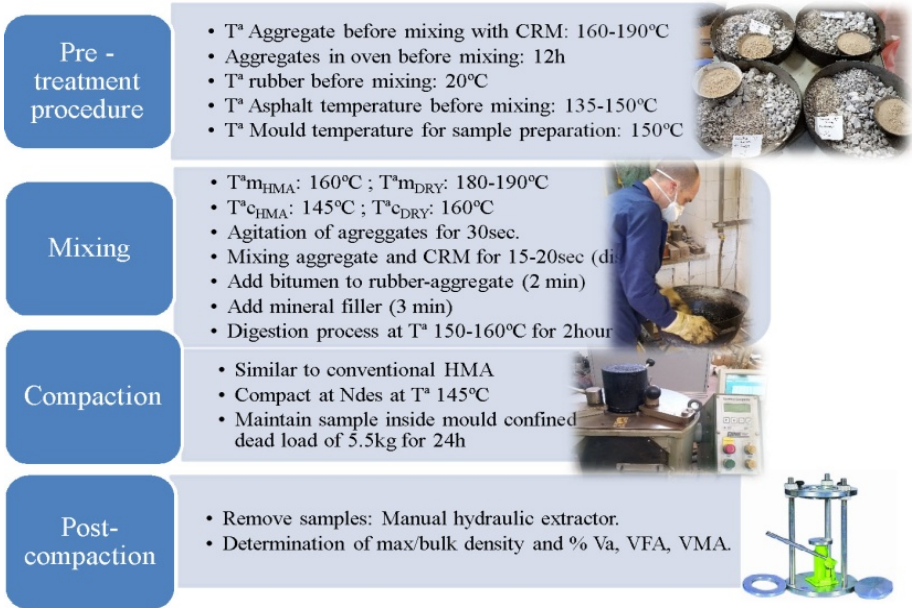

Fig. 21 Construction procedures of dry mixtures.

(a) (b)

Fig. 22 Indirect tensile strength test: (a) test frame and specimen; (b) Marshall and Superpave samples compacted to test for moisture damage.

Table 16 Summary of IDT and ITSR (indirect tensile strength ratio) for HMA reference mixture.

Properties (SG specimens)	DRY	WET	Standard
Indirect tensile strength at 15 ºC (N/mm^2)	1.19	1.40	≥ 0.6
Water sensitivity (ITSR %)	85.2		> 80
Coefficient indirect tensile strength (CTI) at 25 ºC (EN 12697-23, N/mm^2)	123.75	91.84	30-110
Properties (Marshall specimens)	DRY	WET	Standard
Indirect tensile strength at 15 ºC (N/mm^2)	1.32	1.53	≥ 0.6
Water sensitivity (ITSR %)	86.3		> 80
Coefficient indirect tensile strength (CTI) at 25 ºC (EN 12697-23, N/mm^2)	66.09	77.88	30-110

vacuum saturation followed by a 24 hour freeze cycle at 30-40 ºC.

In addition, for the different specimens (4 for each mix) obtained from the workability study, its indirect tensile strength, IDT (indirect tensile strength test) (EN 12697-23) was evaluated because it directly measures the tensile strength in the mixing and cohesion steps. An example, for the reference mix, six test cylinders of diameter 101.6 mm and heights ranging from 35 to 75 mm were subjected to compressive loads between two loading strips at a constant velocity of 50 m/min.

These tests were run at 15 ºC. Each set of specimens were divided in dry/wet groups conditioned to measure the water sensitivity. The ratio of the IDT (%) of the water conditioned subset compared to that of the dry subset is determined (Fig. 22, Table 16).

Water sensitivity test (EN 12697-12) was also conducted for the different mixes in order to evaluate the impact of the rubber on the behaviour of the mixes under the water susceptibility properties for their application in sub-ballast layer.

6. Conclusions

It has been proceeded to the calibration of the model to forecast temperatures of Barber and Crispino, both for the road-railway structures considering the main parameters of pavement temperature, wind speed, precipitation, air temperature, and solar radiation, as controlled by the thermal properties of the pavements.

The verification of the applicability of Barber forecasting model, which is widely used in the field road, to the case of the railway superstructure on the basis of the complete temperature data (so the four seasons), provides to make available an appropriate measure to estimate temperatures in sub-ballast to be used for different weather conditions.

It has been necessary to understand the effects of the various track components to develop a rational structural design method for railroad trackbeds. These factors include axle load, subgrade modulus, etc. A trackbed that has strong load bearing capacity of subgrade should be able to support heavy tonnage and wheel loads without excessive deformation.

KENTRACK has shown to be applicable for calculating stresses and strains in the trackbed and predicting associated design lives for a specific set of design parameters.

An experiment was conducted through SGC to determine N_{des}. Three premises have been achieved, there was a relationship between pavement densification and accumulated traffic, there was a relationship between the densities of samples compacted in the SGC with/without rubber, and there was a linear relationship between N_{design} and rail design traffic.

The SGC has been used to determine an optimal mixture. After that, the global procedure for the mix design was defined and a laboratory verification was conducted. Based on the results, the methodology proposed is considered successful in estimating the optimal ratio binder-voids percentage in the studied case.

A railway equivalent single axle load for the Sicilian traffic has been defined as the rail axle load that produces the same vertical displacement (w) at high temperature (35 °C) and the same horizontal tensile

strain (εt) at low temperature (0 °C) produced by the *ESAL* (80 kN) in the road structure.

The tensile strain was selected at low temperature as the benchmark parameter for the comparison and for the definition of RESAL because it is the critical factor governing cracking and fatigue. The vertical displacement was selected as the benchmark parameter at high temperature because it is the critical factor governing rutting. According to this procedure, the R_{ESAL} has been defined equal to 16 t.

The rubberized mix-results obtained and the comparison with a conventional hot mix asphalt show that these dry rubber bituminous mixtures are particularly effective in damping vibrations. The purpose of using rubber modifiers in HMA to obtain a stiffer-elastic sustainable material has been achieved for the assessment of its behavior in sub-ballast/base layers.

Acknowledgments

The research presented was carried out as part of the Marie Curie Initial Training Network (ITN) action, FP7-PEOPLE-2013-ITN. This project has received funding from the European Union's 7th Framework Program for research, technological development and demonstration under grant agreement number 607524.

Compliance with Ethical Standard

The author(s) declare(s) that there is no potential conflict of interest, also confirm that the manuscript has been read and approved by all named authors and that there are no other persons who satisfied the criteria for authorship but are not listed. We further confirm that the order of authors listed in the manuscript has been approved by all of us and, that we have followed the regulations of our institutions concerning intellectual property.

References

[1] Hidalgo-Signes, C., Martínez-Fernández, P., Garzón-Roca, J., and Insa-Franco, R. 2016. "Analysis of the Bearing Capacity of Unbound Granular Mixtures with Rubber Particles from Scrap Tyres When Used as Sub-ballast." *Mater. Construcc.* 66 (324): e105.

[2] Teixeira, P. F., Ferreira, P. A., López Pita, A., Casas, C., and Bachiller, A. 2009. "The Use of Bituminous Sub-ballast on Future High-Speed Lines in Spain: Structural Design and Economical Impact." *International Journal of Railway* 2 (1): 1-7.

[3] Rose, J. G., and Bryson, S. 2009. "Hot Mix Asphalt Railway Trackbeds: Trackbed Materials, Performance Evaluations, and Significant Implications." Presented at International Conference on Perpetual Pavements 2009, Columbus, Ohio.

[4] Rose, J. G., Teixeira, P. F., and Veit, P. 2011. *International Design Practices, Applications, and Performances of Asphalt/Bituminous Railway Trackbeds.* Paris, France: GEORAIL.

[5] Fang, M., Rose, J. G., West, R. C., Qiu, Y., Ai, C. 2011. "Comparative Analysis on Dynamic Behavior of Two HMA Railway Substructures." *J Transp. Res Board* 19 (1): 26-34.

[6] Esveld, C. 2001. *Modern Railway Track*. Vol. 385. Zaltbommel, the Netherlands: MRT Production.

[7] Sánchez-Borràs, M., and López-Pita, A. 2011. "Rail Infrastructure Charging Systems for High-Speed Lines in Europe." *Transport Reviews* 31 (1): 49-68.

[8] Teixeira, P. F. 2009. "State-of-the-Art on the Use of Bituminous Subballast on European High-Speed Rail Lines. Bearing Capacity of Roads, Railways and Airfields." In *Proceedings of the 8th International Conference on the Bearing Capacity of Roads, Railways and Airfields,* Champaign IL, 29 June.

[9] Sauvage, R., and Larible, G. 1982. "La Modélisation par 'Éléments Finis' des Couches D'assise de la voie Ferrée." *REV GEN CHEM FER* 475-84. (in Italian)

[10] Ramirez Cardona, D. A., Pouget, S., Di Benedetto, H., and Olard, F. 2015. "Viscoelastic Behaviour Characterization of a Gap-Graded Asphalt Mixture with SBS Polymer Modified Bitumen." *Materials Research* 18 (2): 373-81.

[11] Teixeira, P., López-Pita, A., Casas, C., Bachiller, A., and Robuste, F. 2006. "Improvements in High-Speed Ballasted Track Design: Benefits of Bituminous Subballast Layers." *Transportation Research Record: Journal of the Transportation Research Board* 1943: 43-9.

[12] Barber, E. S. 1957. *Calculation of Maximum Pavement Temperatures from Weather Reports*. Highway Research Board Bulletin, 168.

[13] Straub, A. L., Schenck Jr, H. N., and Przbycien, F. E. 1968. "Bituminous Pavement Temperature Related to Climate." *Highway Research Record* 256: 53-77.

[14] Williamson, R. H. 1972. "Effects of Environment on Pavement Temperatures." In *International Conference on Structural Design Proceedings,* 144-58.

[15] Velasquez, R., Marasteanu, M., Clyne, T. R., Engineer, M. F., and Worel, B. 2008. "Improved Model to Predict Flexible Pavement Temperature Profile." Presented at Third International Conference on Accelerated Pavement Testing, Madrid, Spain.

[16] Asphalt Institute. 1982. *Research and Development of the Asphalt Institute's Thickness Design Manual (MS-1).* Research Report 82-2. 9th ed. Asphalt Institute.

[17] Diefenderfer, B., Al-Qadi, I., and Diefenderfer, S. 2006. "Model to Predict Pavement Temperature Profile: Development and Validation." *Journal of Transportation Engineering* 132 (2): 162-7.

[18] Di Mascio, P., and Moretti, L. 2013. "Model for Estimating Temperatures in Concrete Pavements." In *Proceedings of the first International Journal of Pavements Conference, Brazil,* Paper 202-1.

[19] Sol-Sánchez, M., Thom, N. H., Moreno-Navarro, F., Rubio-Gámez, M. C., and Airey, G. D. 2015. "A study into the Use of Crumb Rubber in Railway Ballast." *Construction and Building Materials* 75: 19-24.

[20] Marchionna, M. C., Fornaci, M. G., and Malgarini, M. 1985. *Modello di Degradazione Strutturale Delle Pavimentazioni.* Autostrade 1/85. (in Italian)

[21] Naude, F., Fröhling, R., and Theron, N. 2005. "Development of a Methodology to Calculate Stresses in Track Components." In *Proceedings of the Institution of Mechanical Engineers, Part F: Journal of Rail and Rapid Transit* 219 (4): 213-24.

[22] Hermansson, A. 2001. "Mathematical Model for Calculation of Pavement Temperatures: Comparison of Calculated and Measured Temperatures." *Journal of the Transportation Research Board* 1764: 180-8.

[23] Ferreira, T. M., and Teixeira, P. F. 2012. "Rail Track Performance with Different Subballast Solutions: Traffic and Environmental Effects on Subgrade Service Life." *Journal of Transportation Engineering* 138 (12): 1541-50.

[24] Di Mascio, P., and D'Andrea, A. 1999. "Metodologia Razionale per il Dimensionamento Delle Pavimentazioni Aeroportuali." Presented at Pianificazione e Gestione di Infrastrutture Ferroviarie e Aeroportuali Atti del IX Convegno Nazionale SIIV—Cagliari, vol. 28, p. 29.

[25] Crispino, M. 2001. "Valutazione Delle Temperature in Esercizio del Subballast Ferroviario." *Ingegneria Ferroviaria* (12/2001): 1-2, 30-6. (in Italian)

[26] Crispino, M., Festa, B., and Giannattasio, P. 1998. "Valutazione Delle Temperature Della Sovrastruttura Ferroviaria per alta Velocità Attraverso una Sperimentazione di Laboratorio." Presented at CIFI Congress: La Tecnologia del Trasporto su Ferro e L'Orientamento al Mercato, Napoli. (in Italian)

[27] Martinez-Soto, F., Di Mino, G., and Acuto, F. 2017. *Effect of Temperature and Traffic on Mix-Design of Bituminous Asphalt for Railway Sub-ballast Layer*. BCRRA2017 Conference Proceedings. Athens, Greece: CRC Press—Taylor & Francis Group.

[28] Huang, Y. H., Rose, J. G., and Khoury, C. J. 1987. "Thickness Design for Hot-Mix Asphalt Railroad Trackbeds." *Annual Journal AAPT, Miscellaneous* 56 (87): 427-53.

[29] Yoder, E. J., and Witczak, M. W. 1975. *Principles of Pavement Design.* San Francisco, CA: John Wiley & Sons.

[30] Burmister, D. M. 1943. "Theory of Stresses and Displacements in Layered Systems and Application to the Design of Airport Runways." In *Proceedings of the 23rd Annual Meeting of the Highway Research Board,* 126-48.

[31] Huang, Y. H., Lin, C., and Deng, X. 1984. "Hot Mix Asphalt for Railroad Trackbeds-Structural Analysis and Design." *Asphalt Paving Technology* 53: 475.

[32] Huang, Y. H., Lin, C., Deng, X., and Rose, J. 1984. *Kentrack: A Computer Program for Hot-Mix Asphalt and Conventional Ballast Railway Trackbed.* Maryland (USA)*:* Asphalt Institute.

[33] Huang, Y. H. 1993. *Pavement Analysis and Design*. NJ, USA: Englewood Cliffs.

[34] Rose, J. G., Liu, S., and Souleyrette, R. R. 2014. "KENTRACK 4.0: A Railway Trackbed Structural Design Program." Presented at 2014 Joint Rail Conference. American Society of Mechanical Engineers.

[35] Rose, J., Liu, S., and Souleyrette, R. R. 2014. "Kentrack 4.0: A Railway Trackbed Structural Design Program." In *Proceedings of the 2014 Joint Rail Conference JRC 2014,* April 2-4, 2014, Colorado Springs, Colorado, USA.

[36] Rose, J. G., Agarwal, N. K., Brown, J. D., and Ilavala, N. 2010. "KENTRACK, A Performance-Based Layered Elastic Railway Trackbed Structural Design and Analysis Procedure–A Tutorial." In *Proceedings of the 2010 Joint Rail Conference,* 73-110.

[37] Liu, S. 2013. "KENTRACK 4.0: A Railway Trackbed Structural Design Program." Thesis, University of Kentucky.

[38] McHenry, M. T., and Rose, J. G. 2012. *Railroad Subgrade Support and Performance Indicators: A Review of Available Laboratory and In-situ Testing Methods.* Research report of University of Kentucky.

[39] RFI (Rete Ferroviaria Italiana). 2016. *Gruppo Ferrovie dello Stato Italiane.* Capitolato Costruzioni Opere Civili. Sezione XV Sub-ballast—Pavimentazioni Stradali. (in Italian)

[40] Di Mascio, P., Loprencipe, G., and Moretti, L. 2014. "Competition in Rail Transport: Methodology to Evaluate Economic Impact of New Trains on Track." Presented at the 3rd International Conference on Transportation Infrastructure ICTI2014, Pisa, 22-5.

[41] Sadeghi, J., and Barati, P. 2010. "Evaluation of Conventional Methods in Analysis and Design of Railway Track System." *International Journal of Civil Engineering* 8 (1): 44-55.

[42] Rose, J. G., and Konduri, K. C. 2006. "A Railway Trackbed Structural Design Program." In *Proceedings of the American Railway Engineering and Maintenance of Way Annual Conference.* Louisville, Kentucky. September 2008.

[43] Rose, J., Su, B., and Twehues, F. 2004. "Comparisons of Railroad Track and Substructure Computer Model Predictive Stress Values and In-situ Stress Measurements." Presented at Annual Conf. and Exposition, American Railway Engineering and Maintenance-of-Way Association (AREMA), Nashville.

[44] Andrei, D., Witczak, M. W., and Mirza, M. W. 1999. *Development of a Revised Predictive Model for the Dynamic (Complex) Modulus of Asphalt Mixtures.* NCHRP 1-37A Interim Team Report, University of Maryland.

[45] Cardona, D. R., Di Benedetto, H., Sauzeat, C., Calon, N., and Saussine, G. 2016. "Use of a Bituminous Mixture Layer in High-Speed Line Trackbeds." *Construction and Building Materials* 125: 398-407.

[46] Bari, J., and Witczak, M. W. 2006. "Development of a New Revised Version of the Witczak E* Predictive Model of Hot Mix Asphalt Mixtures." *Journal of the Association of Asphalt Paving Technologist* 75: 381-424.

[47] NCHRP (National Cooperative Highway Research Program). 2007. *Superpave Mix Design: Verifying Gyration Levels in the N_{design} Table.* Report 573.

[48] Witczak, M. W., Kaloush, K., Pellinen, T., El-Basyouny, M., and Von Quintus, H. 2002. *Simple Performance Test for Superpave Mix Design.* NCHRP Report 465, Transportation Research Board, Washington, D.C.

[49] AASHTO (American Association of State Highway and Transportation Officials). 2001. *Superpave Volumetric Design for Asphalt Mixtures.* AASHTO R 35-151, 444 North Capitol Street N.W., Suite 249 Washington, D.C.

[50] Hassan, N. A., Airey, G. D., Jaya, R. P., and Aziz, M. A. 2014. "A Review of Crumb Rubber Modification in Dry Mixed Rubberised Asphalt Mixtures." *Jurnal Teknologi* 70 (4): 127-34.

[51] ASTM D2493/D2493M. 2009. *Standard Viscosity-Temperature Chart for Asphalts.* D04.44, Book of Standards Volume: 04.03, ASTM International, USA.